CLIMATE DIAGNOSTICS BULLETIN



JUNE 2009

NEAR REAL-TIME OCEAN / ATMOSPHERE

Monitoring, Assessments, and Prediction

U.S. DEPARTMENT OF COMMERCE National Oceanic and Atmospheric Administration National Weather Service National Centers for Environmental Prediction

CLIMATE DIAGNOSTICS BULLETIN



CLIMATE PREDICTION CENTER Attn: Climate Diagnostics Bulletin W/NP52, Room 605, WWBG Camp Springs, MD 20746-4304

Chief Editor: Gerald D. Bell **Editors:** Wei Shi, Michelle L'Heureux, and Michael Halpert **Bulletin Production:** Wei Shi

ExternalCollaborators:

Center for Ocean-Atmospheric Prediction Studies (COAPS) Cooperative Institute for Research in the Atmosphere (CIRA) Earth & Space Research International Research Institute for Climate and Society (IRI) Joint Institute for the Study of the Atmosphere and Ocean (JISAO) Lamont-Doherty Earth Observatory (LDEO) NOAA-CIRES, Climate Diagnostics Center NOAA-AOML, Atlantic Oceanographic and Meteorological Laboratory NOAA-NESDIS-STAR, Center for Satellite Applications and Research NOAA-NDBC, National Data Buoy Center Scripps Institution of Oceanography

Software: Most of the bulletin figures generated at CPC are created using the Grid Analysis and Display System (GrADS).

- Climate Diagnostics Bulletin available on the World Wide Web

The CDB is available on the World Wide Web. The address of the online version of the CDB is:

http://www.cpc.ncep.noaa.gov/products/CDB

If you have any problems accessing the bulletin, contact Dr. Wei Shi by E-mail:

Wei.Shi@noaa.gov

Table of Contents

TROPICS

Highlights page 6	
Table of Atmospheric Indices page 7	
Table of Oceanic Indices page 8	

FIGURE

Time Series	
Southern Oscillation Index (SOI)	T1
Tahiti and Darwin SLP Anomalies	T1
OLR Anomalies	T1
CDAS/Reanalysis SOI & Equatorial SOI	Τ2
200-hPa Zonal Wind Anomalies	Т3
500-hPa Temperature Anomalies	Т3
30-hPa and 50-hPa Zonal Wind Anomalies	Т3
850-hPa Zonal Wind Anomalies	T4
Equatorial Pacific SST Anomalies	Т5
Time-Longitude Sections	
Mean and Anomalous Sea Level Pressure	Т6
Mean and Anomalous 850-hPa Zonal Wind	Τ7
Mean and Anomalous OLR	Т8
Mean and Anomalous SST	Т9
Pentad SLP Anomalies	T10
Pentad OLR Anomalies	T11
Pentad 200-hPa Velocity Potential Anomalies	T12
Pentad 850-hPa Zonal Wind Anomalies	T13
Anomalous Equatorial Zonal Wind	T14
Mean and Anomalous Depth of the 20°C Isotherm	T15
Mean & Anomaly Fields	
Depth of the 20°C Isotherm	T16
Subsurface Equatorial Pacific Temperatures	T17
SST	T18
SLP	T19
850-hPa Vector Wind	T20
200-hPa Vector Wind	T21
200-hPa Streamfunction	T22
200-hPa Divergence	T23
200-hPa Velocity Potential and Divergent Wind	T24
OLR	T25
SSM/I Tropical Precipitation Estimates	T26
Cloud Liquid Water	T27
Precipitable Water	T28
Divergence & E-W Divergent Circulation	T29 - T30
Pacific Zonal Wind & N-S Divergent Circulation	T31-T32

Appendix 1: Outside Contributions

Tropical Drifting Buoys	A1.1
Thermistor Chain Data	A1.2
TAO/TRITON Array Time-Longitude Sections	A1.3 - A1.4

FIGURE

East Pacific SST and Sea Level	A1.5
Pacific Wind Stress and Anomalies	A1.6
Satellite-Derived Surface Currents	A1.7 - A1.8

FORECAST FORUM

Discussion page 49

F1 - F2
F3 - F4
F5 - F6
F7 - F8
F9 - F10
F11
F12
F13

EXTRATROPICS

Highlights page 64	
Table of Teleconnection Indices page 66	
Global Surface Temperature	E1
Temperature Anomalies (Land Only)	E2
Global Precipitation	E3
Regional Precipitation Estimates	E4 - E5
U. S. Precipitation	E6
Northern Hemisphere	
Teleconnection Indices	E7
Mean and Anomalous SLP	E8
Mean and Anomalous 500-hPa heights	E9
Mean and Anomalous 300-hPa Wind Vectors	E10
500-hPa Persistence	E11
Time-Longitude Sections of 500-hPa Height Anomalies	E12
700-hPa Storm Track	E13
Southern Hemisphere	
Mean and Anomalous SLP	E14
Mean and Anomalous 500-hPa heights	E15
Mean and Anomalous 300-hPa Wind Vectors	E16
500-hPa Persistence	E17
Time-Longitude Sections of 500-hPa Height Anomalies	E18
Stratosphere	
Height Anomalies	S1 - S2
Temperatures	S3 - S4
Ozone	S5 - S6
Vertical Component of EP Flux	S7
Ozone Hole	S8
Appendix 2: Additional Figures	
Arctic Oscillation and 500-hPa Anomalies	A2.1
Snow Cover	A2.2

Tropical Highlights - June 2009

Sea surface temperature (SST) anomalies continued to increase across the equatorial Pacific Ocean during June 2009(**Fig. T18**). The latest monthly SST index was $+0.6^{\circ}$ C in the Niño-3.4 region, and $+0.7^{\circ}$ C in the Niño-1+2 region (**Table T2, Fig. T5**).

The oceanic thermocline along the equator, measured by the depth of the 20°C isotherm, remained deeper than average across the equatorial Pacific Ocean during June (**Figs. T15, T16**). Consistent with these conditions, temperatures were 1°-3°C above average at thermocline depth across the equatorial Pacific (**Fig. T17**).

Also during June, the low-level equatorial easterly winds (**Fig. T20**, **Table T1**) were weaker than average across the central and eastern equatorial Pacific Ocean, and convection became increasingly suppressed over Indonesia (**Figs. T25**, **E3**). This coupling of the oceanic and atmospheric anomalies indicates the development of El Niño.

For the latest status of the ENSO cycle see the ENSO Diagnostic Discussion at: http://www.cpc.ncep.noaa.gov/products/analysis_monitoring/enso_advisory/index.html

HLNOW	SLP ANOM	OMALIES	TAHITI Tainus TAMTN	850-hP;	850-hPa ZONAL WIND INDEX	(D INDEX	200-hPa WIND INDEX	OLR Index
	ITIHAT	DARWIN	SOI	5N-5S 135E-180	5N-5S 175W-140W	5N-5S 135W-120W	5N-5S 165W-110W	5N-5S 160E-160W
60 NN	-0.1	0.4	-0.3	0.2	-0.5	-1.5	-0.4	0.3
MAY 09	-0.9	-0.3	-0.4	9.0	0.2	-0.4	-0.3	0.8
APR 09	0.9	-0.1	0.7	1.5	0.8	0.2	0.3	1.0
MAR 09	0.9	1.1	-0.1	0.8	0.7	0.0	1.5	1.4
FEB 09	1.7	-1.2	1.8	3.0	1.4	-0.1	1.9	1.7
JAN 09	1.6	-0.2	1.2	2.0	6.0	-0.8	0.9	1.8
DEC 08	1.6	-0.8	1.5	2.5	1.4	-0.4	2.0	2.3
NOV 08	1.7	-0.6	1.5	3.4	1.4	-0.1	1.5	1.2
OCT 08	2.4	0.4	1.3	2.1	0.4	-1.0	-0.2	1.1
SEP 08	2.1	-0.2	1.5	1.2	0.4	-0.5	0.4	0.3
AUG 08	2.1	0.9	0.8	1.8	0.1	-1.2	0.0	0.7
JUL 08	0.8	0.6	0.2	2.0	0.1	-1.2	0.1	0.9
JUN 08	1.2	0.8	0.3	1.7	0.5	-1.1	0.5	0.4
	- - -	- - -			;	;	,	

TABLE T1 - Atmospheric index values for the most recent 12 months. Indices are standardized by the mean annual standard deviation, except for the Tahiti and Darwin SLP anomalies which are in units of hPa. Positive (negative) values of 200-hPa zonal wind index imply westerly (easterly) anomalies. Positive (negative) values of 850-hPa zonal wind indices imply easterly (westerly) anomalies.

				PACIFIC	IC SST				Ā	ATLANTIC	IC SST	F	Glo	Global
MONTH	N IŇ C 0-1 90°W	NIÑO 1+2 0-10°S 90°W-80°W	N IÑ O 5 ° N - 5 ° 150 ° W -	NIÑO 3 5°N-5°S 50°W-90- °W	NIÑO 3.4 5°N-5°S 170°W-12 0°W	NIÑO 3.4 5°N-5°S 70°W-12- 0°W	NIÑ0 4 5°N-5°S 160°E-15 °W	0 4 -5°S :-150- V	N. ATL 5N-20N 60W-30W	N. ATL 5N-20N 0W-30W	S 0-2 30W	S. ATL 0-20S 30W-10E	TRO 10N-30W-3	TR OPIC S 10N-10S 0W-360W
60 NUL	0.7	23.7	0.7	27.1	0.6	28.1	0.6	29.2	-0.1	26.6	0.5	25.3	0.5	28.3
MAY 09	0.6	24.9	0.4	27.4	0.3	28.0	0.3	29.0	-0.2	26.0	6.0	26.9	0.4	28.7
APR 09	0.5	26.0	0.0	27.4	-0.2	27.5	0.0	28.4	0.1	25.8	0.7	27.5	0.2	28.6
MAR 09	-0.1	26.4	-0.6	26.4	-0.5	26.7	-0.3	27.8	0.0	25.4	0.6	27.5	0.0	28.2
FEB 09	-0.1	26.0	-0.6	25.8	-0.7	26.0	-0.7	27.4	0.0	25.4	0.3	26.7	0.0	27.7
1AN 09	-0.2	24.3	-0.6	25.0	- 1.0	25.5	-0.7	27.4	0.4	26.3	0.3	25.7	0.0	27.5
DEC 08	-0.4	22.4	-0.5	24.6	-0.7	25.7	-0.6	27.7	0.6	27.2	0.4	24.9	0.1	27.5
NOV 08	-0.2	21.5	-0.2	24.8	-0.2	26.3	-0.3	28.1	0.6	28.0	0.1	24.0	0.1	27.6
OCT 08	-0.2	20.8	-0.1	24.8	-0.3	26.3	-0.1	28.3	0.7	28.6	0.2	23.5	0.2	27.5
SEP 08	0.7	21.2	0.3	25.1	-0.2	26.5	-0.4	28.1	0.7	28.6	0.2	23.1	0.2	27.3
AUG 08	1.1	21.9	0.7	25.7	0.2	26.9	-0.3	28.2	0.5	28.0	0.5	23.5	0.2	27.3
JUL 08	0.8	22.7	0.6	26.1	0.1	27.2	-0.3	28.3	0.3	27.4	0.6	24.2	0.1	27.4
30 NUC	0.6	23.7	0.2	26.6	-0.3	27.2	-0.6	28.1	0.2	26.8	0.7	25.5	0.0	27.9

TABLE T2. Mean and anomalous sea surface temperature (°C) for the most recent 12 months. Anomalies are departures from the 1971–2000 adjusted OI climatology (Smith and Reynolds 1998, *J. Climate*, **11**, 3320-3323).

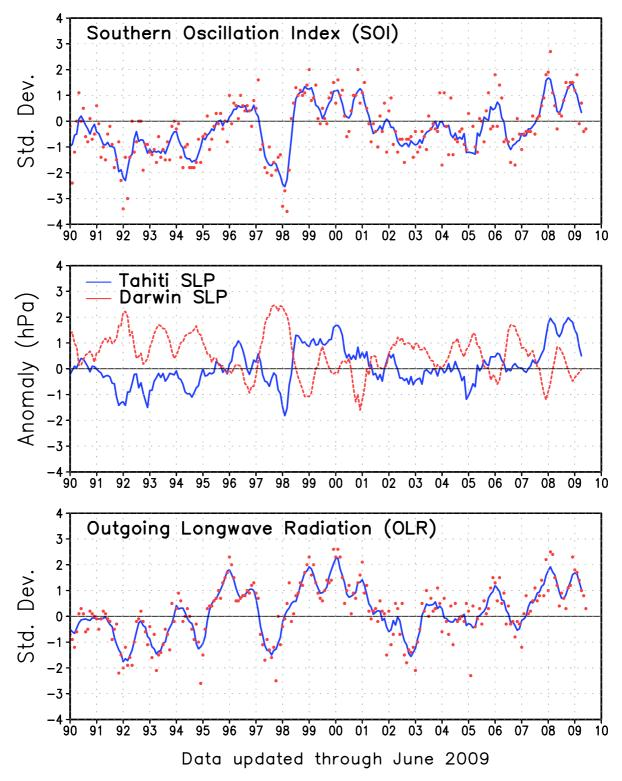


FIGURE T1. Five-month running mean of the Southern Oscillation Index (SOI) (top), sea-level pressure anomaly (hPa) at Darwin and Tahiti (middle), and outgoing longwave radiation anomaly (OLR) averaged over the area 5N-5S, 160E-160W (bottom). Anomalies in the top and middle panels are departures from the 1951-1980 base period means and are normalized by the mean annual standard deviation. Anomalies in the bottom panel are departures from the 1979-1995 base period means. Individual monthly values are indicated by "x"s in the top and bottom panels. The x-axis labels are centered on July.

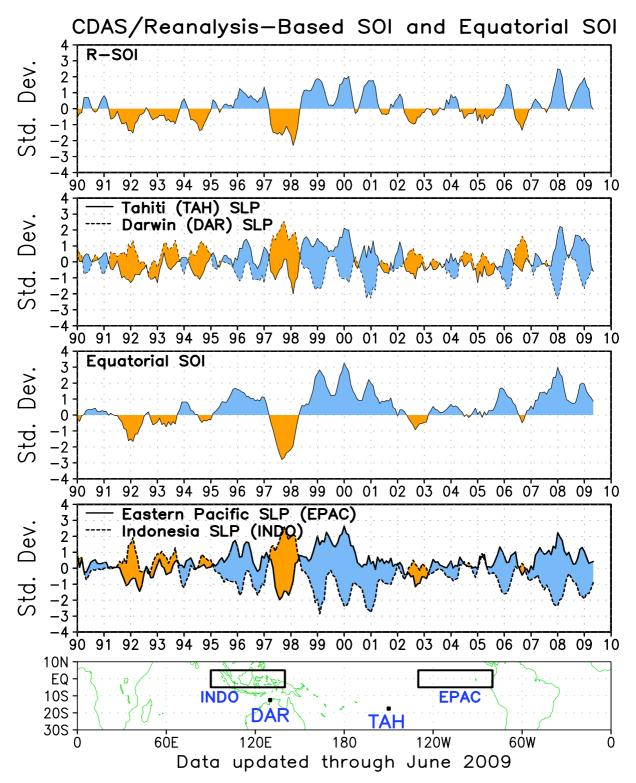


FIGURE T2. Three-month running mean of a CDAS/Reanalysis-derived (a) Southern Oscillation Index (RSOI), (b) standardized pressure anomalies near Tahiti (solid) and Darwin (dashed), (c) an equatorial SOI ([EPAC] - [INDO]), and (d) standardized equatorial pressure anomalies for (EPAC) (solid) and (INDO) (dashed). Anomalies are departures from the 1979–95 base period means and are normalized by the mean annual standard deviation. The equatorial SOI is calculated as the normalized difference between the standardized anomalies averaged between 5°N–5°S, 80°W–130°W (EPAC) and 5°N–5°S, 90°E–140°E (INDO).

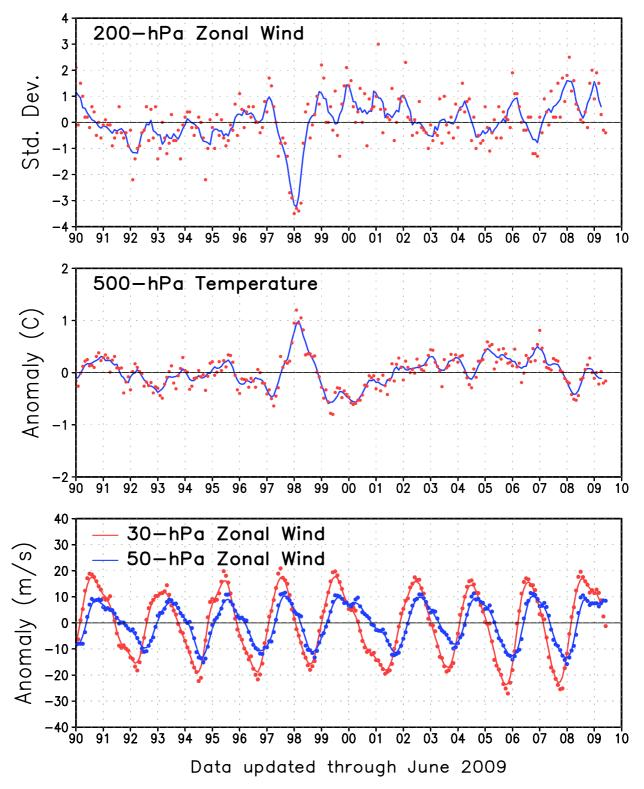


FIGURE T3. Five-month running mean (solid lines) and individual monthly mean (dots) of the 200-hPa zonal wind anomalies averaged over the area 5N-5S, 165W-110W (top), the 500-hPa virtual temperature anomalies averaged over the latitude band 20N-20S (middle), and the equatorial zonally-averaged zonal wind anomalies at 30-hPa (red) and 50-hPa (blue) (bottom). In the top panel, anomalies are normalized by the mean annual standard deviation. Anomalies are departures from the 1979-1995 base period means. The x-axis labels are centered on January.

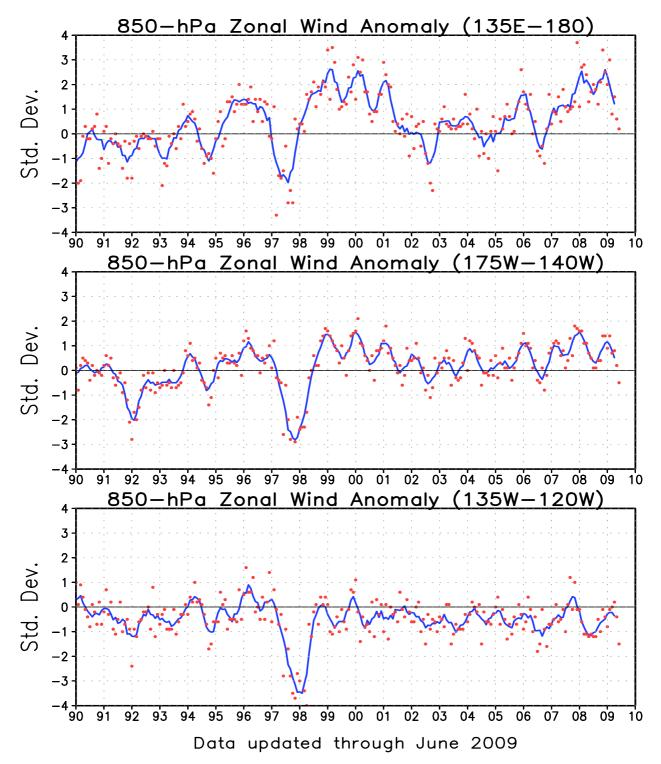


FIGURE T4. Five-month running mean (solid line) and individual monthly mean (dots) of the standardized 850-hPa zonal wind anomaly index in the latitude belt 5N-5S for 135E-180 (top), 175W-140W (middle) and 135W-120W (bottom). Anomalies are departures from the 1979-1995 base period means and are normalized by the mean annual standard deviation. The x-axis labels are centered on January. Positive (negative) values indicate easterly (west-erly) anomalies.

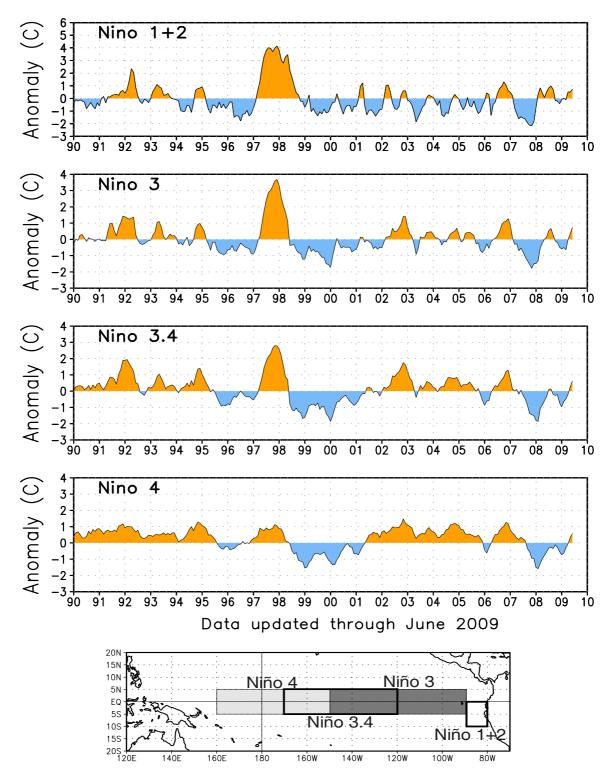


FIGURE T5. Nino region indices, calculated as the area-averaged sea surface temperature anomalies (C) for the specified region. The Nino 1+2 region (top) covers the extreme eastern equatorial Pacific between 0-10S, 90W-80W. The Nino-3 region (2nd from top) spans the eastern equatorial Pacific between 5N-5S, 150W-90W. The Nino 3.4 region 3rd from top) spans the east-central equatorial Pacific between 5N-5S, 170W-120W. The Nino 4 region (bottom) spans the date line and covers the area 5N-5S, 160E-150W. Anomalies are departures from the 1971-2000 base period monthly means (*Smith and Reynolds 1998, J. Climate, 11, 3320-3323*). Monthly values of each index are also displayed in Table 2.

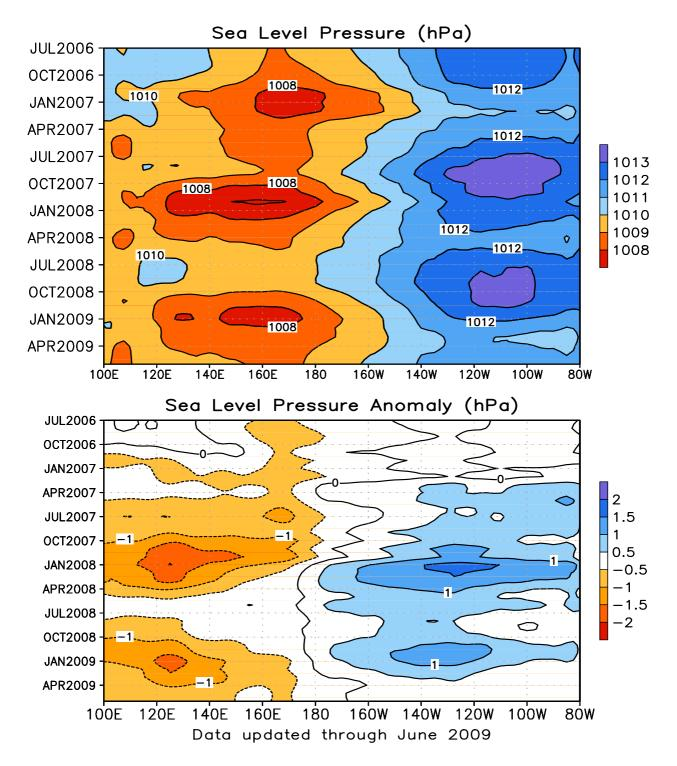


FIGURE T6. Time-longitude section of mean (top) and anomalous (bottom) sea level pressure (SLP) averaged between 5N-5S (CDAS/Reanalysis). Contour interval is 1.0 hPa (top) and 0.5 hPa (bottom). Dashed contours in bottom panel indicate negative anomalies. Anomalies are departures from the 1979-1995 base period monthly means. The data are smoothed temporally using a 3-month running average.

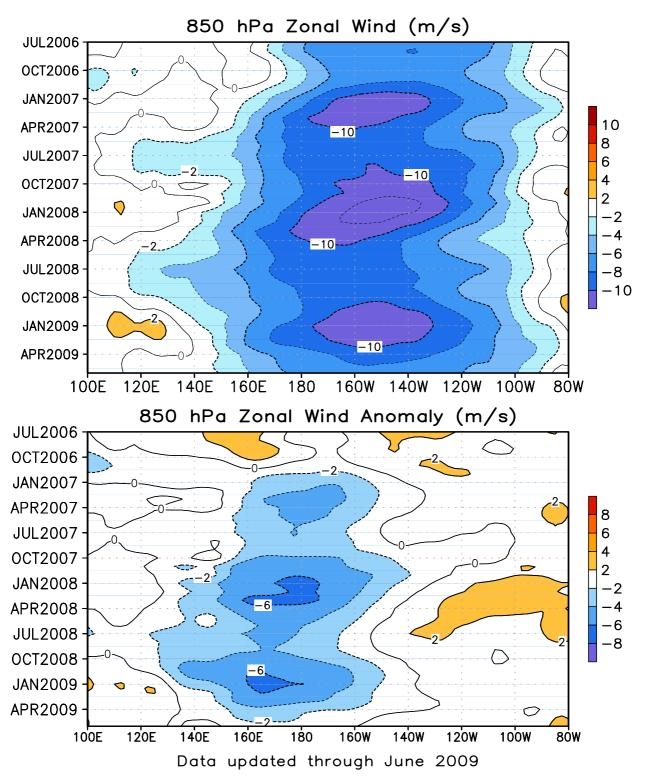


FIGURE T7. Time-longitude section of mean (top) and anomalous (bottom) 850-hPa zonal wind averaged between 5N-5S (CDAS/Reanalysis). Contour interval is 2 ms⁻¹. Blue shading and dashed contours indicate easterlies (top) and easterly anomalies (bottom). Anomalies are departures from the 1979-1995 base period monthly means. The data are smoothed temporally using a 3-month running average.

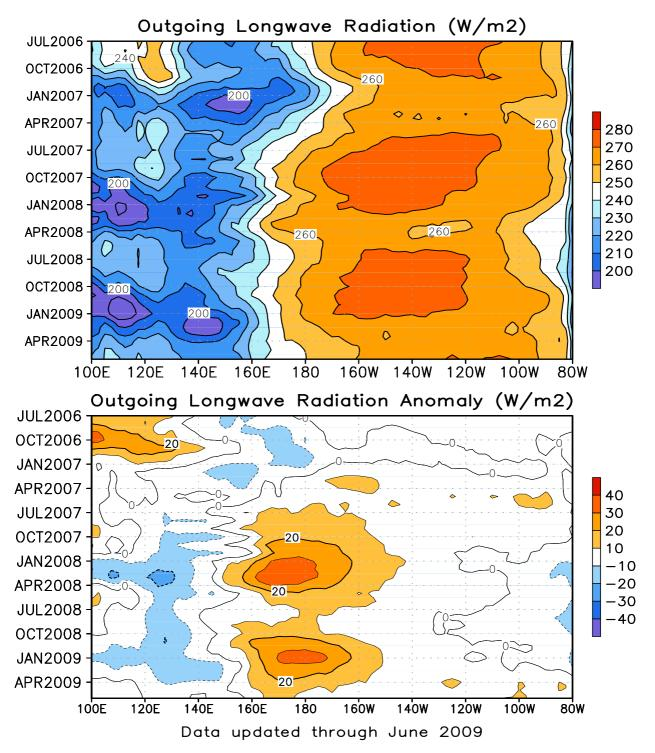


FIGURE T8. Time-longitude section of mean (top) and anomalous (bottom) outgoing longwave radiation (OLR) averaged between 5N-5S. Contour interval is 10 Wm⁻². Dashed contours in bottom panel indicate negative OLR anomalies. Anomalies are departures from the 1979-1995 base period monthly means. The data are smoothed temporally using a 3-month running average.

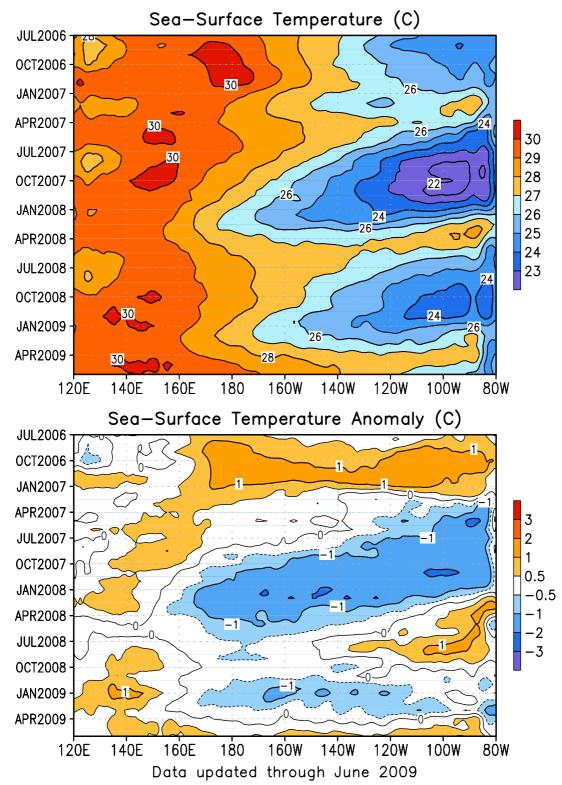


FIGURE T9. Time-longitude section of monthly mean (top) and anomalous (bottom) sea surface temperature (SST) averaged between 5N-5S. Contour interval is 1C (top) and 0.5C (bottom). Dashed contours in bottom panel indicate negative anomalies. Anomalies are departures from the 1971-2000 base period means (Smith and Reynolds 1998, *J. Climate*, **11**, 3320-3323).

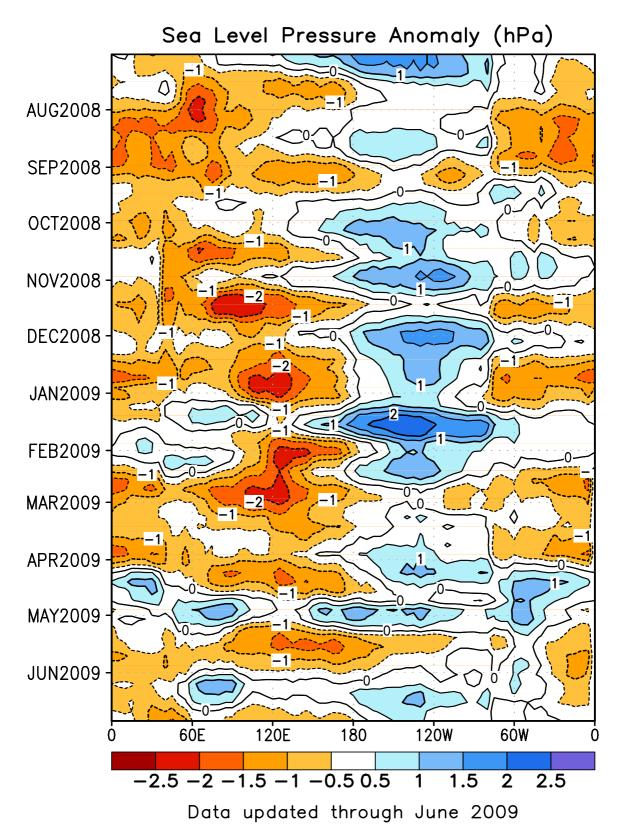


FIGURE T10. Time-longitude section of anomalous sea level pressure (hPa) averaged between 5N-5S (CDAS/Reanaysis). Contour interval is 1 hPa. Dashed contours indicate negative anomalies. Anomalies are departures from the 1979-1995 base period pentad means. The data are smoothed temporally using a 3-point running average.

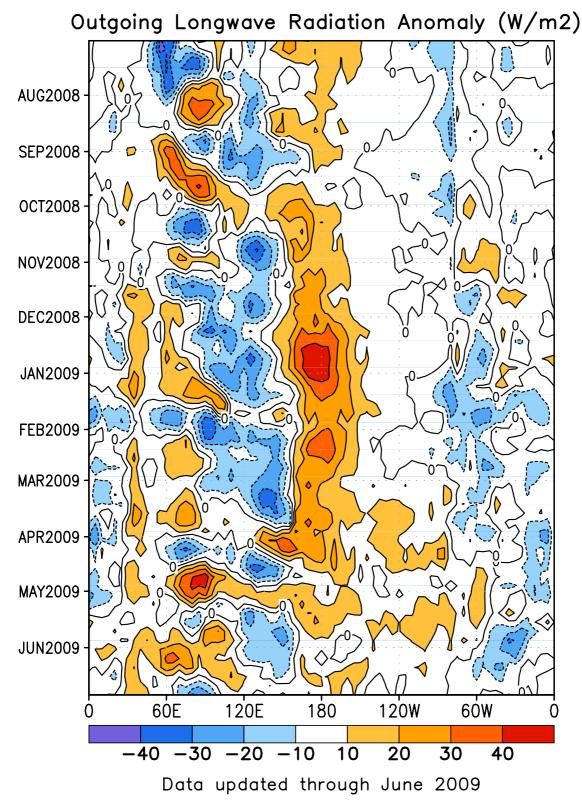


FIGURE T11. Time-longitude section of anomalous outgoing longwave radiation averaged between 5N-5S. Contour interval is 15 Wm⁻². Dashed contours indicate negative anomalies. Anomalies are departures from the 1979-1995 base period pentad means. The data are smoothed temporally using a 3-point running average.

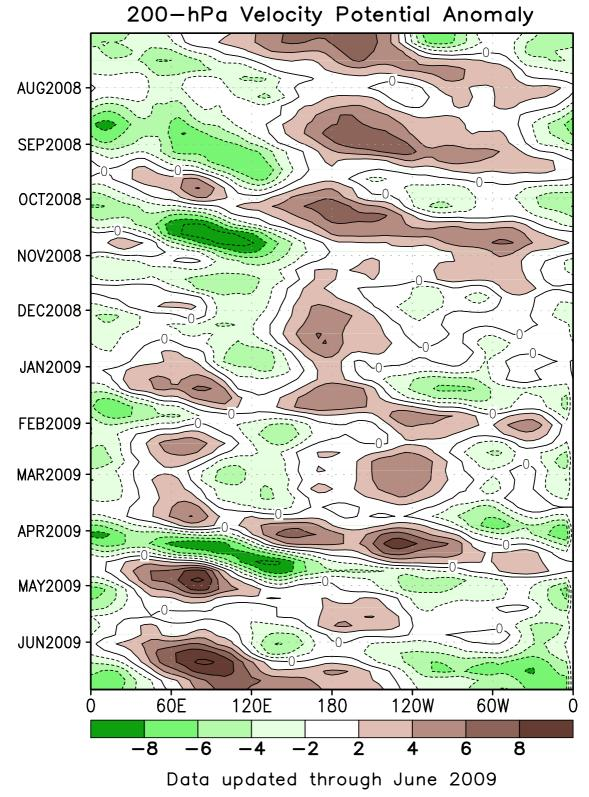


FIGURE T12. Time-longitude section of anomalous 200-hPa velocity potential averaged between 5N-5S (CDAS/Reanalysis). Contour interval is 3 x 10⁶ m²s⁻¹. Dashed contours indicate negative anomalies. Anomalies are departures from the 1979-1995 base period pentad means. The data are smoothed temporally using a 3-point running average.

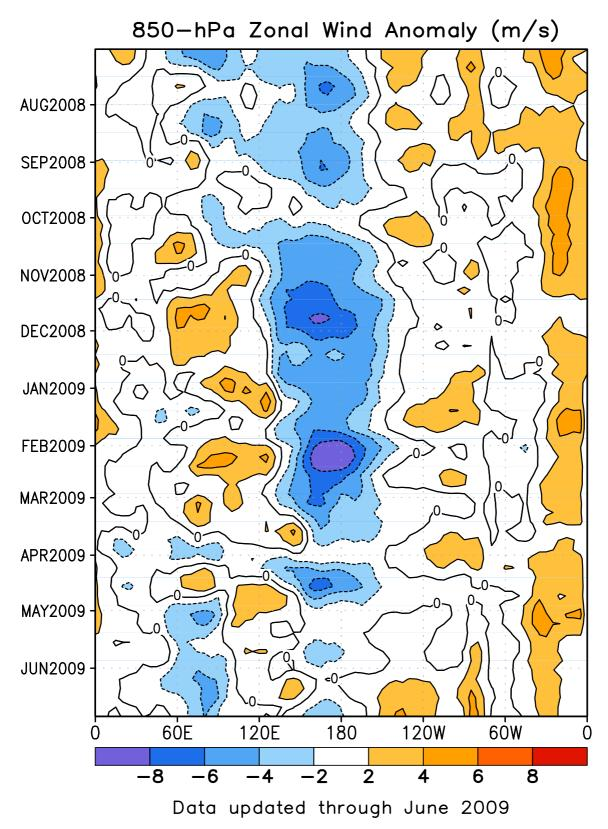


FIGURE T13. Time-longitude section of anomalous 850-hPa zonal wind averaged between 5N-5S (CDAS/Reanalysis). Contour interval is 2 ms⁻¹. Dashed contours indicate negative anomalies. Anomalies are departures from the 1979-1995 base period pentad means. The data are smoothed temporally by using a 3-point running average.

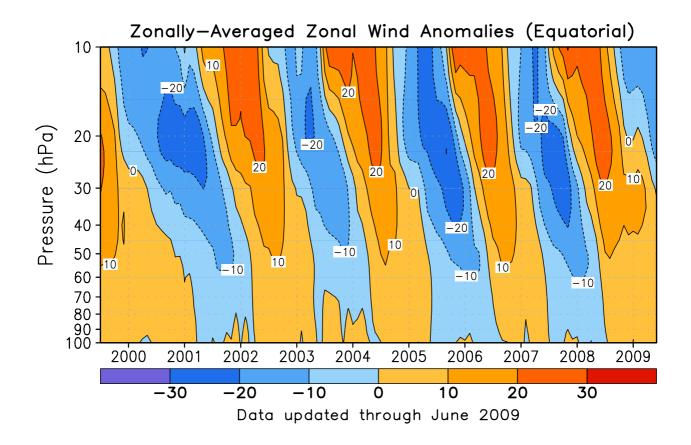


FIGURE T14. Equatorial time-height section of anomalous zonally-averaged zonal wind (m s⁻¹) (CDAS/Reanalysis). Contour interval is 10 ms⁻¹. Anomalies are departures from the 1979-1995 base period monthly means.

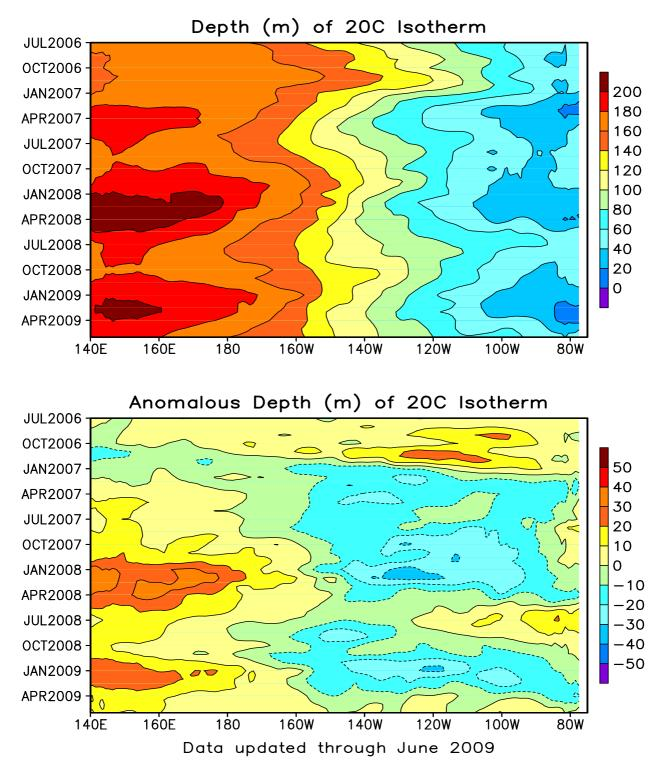


FIGURE T15. Mean (top) and anomalous (bottom) depth of the 20C isotherm averaged between 5N-5S in the Pacific Ocean. Data are derived from the NCEP's global ocean data assimilation system which assimilates oceanic observations into an oceanic GCM (Behringer, D. W., and Y. Xue, 2004: Evaluation of the global ocean data assimilation system at NCEP: The Pacific Ocean. AMS 84th Annual Meeting, Seattle, Washington, 11-15). The contour interval is 10 m. Dashed contours in bottom panel indicate negative anomalies. Anomalies are departures from the 1982-2004 base period means.

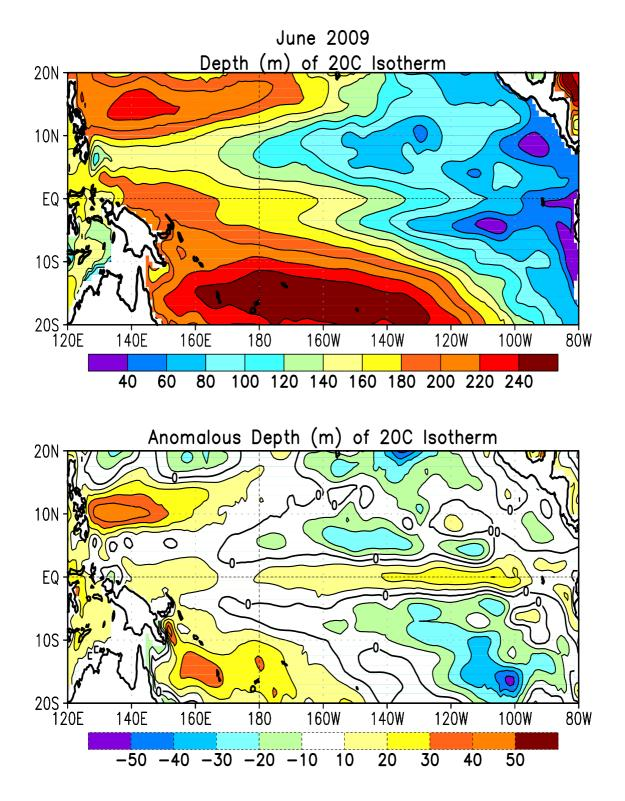


FIGURE T16. Mean (top) and anomalous (bottom) depth of the 20°C isotherm for JUN 2009. Contour interval is 40 m (top) and 10 m (bottom). Dashed contours in bottom panel indicate negative anomalies. Data are derived from the NCEP's global ocean data assimilation system version 2 which assimilates oceanic observations into an oceanic GCM (Xue, Y. and Behringer, D.W., 2006: Operational global ocean data assimilation system at NCEP, to be submitted to BAMS). Anomalies are departures from the 1982–2004 base period means.

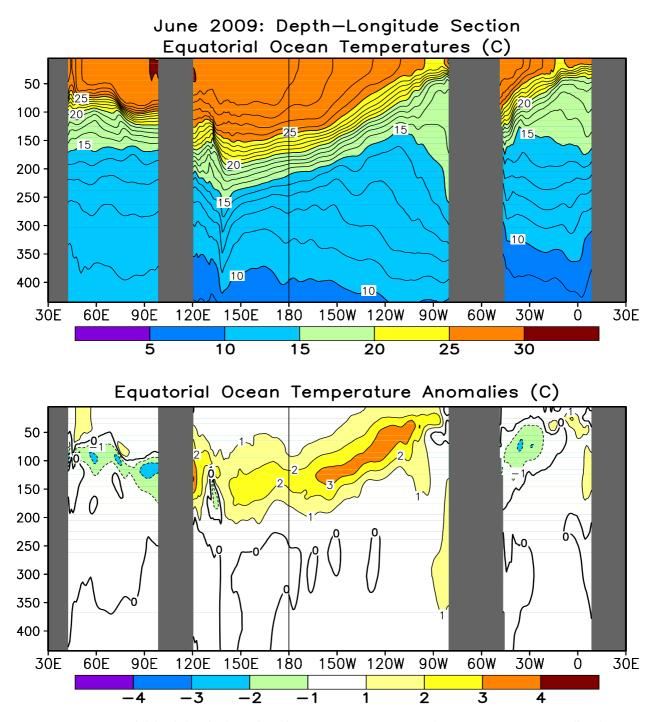


FIGURE T17. Equatorial depth-longitude section of ocean temperature (top) and ocean temperature anomalies (bottom) for JUN 2009. Contour interval is 1°C. Dashed contours in bottom panel indicate negative anomalies. Data are derived from the NCEP's global ocean data assimilation system version 2 which assimilates oceanic observations into an oceanic GCM (Xue, Y. and Behringer, D.W., 2006: Operational global ocean data assimilation system at NCEP, to be submitted to BAMS). Anomalies are departures from the 1982–2004 base period means.

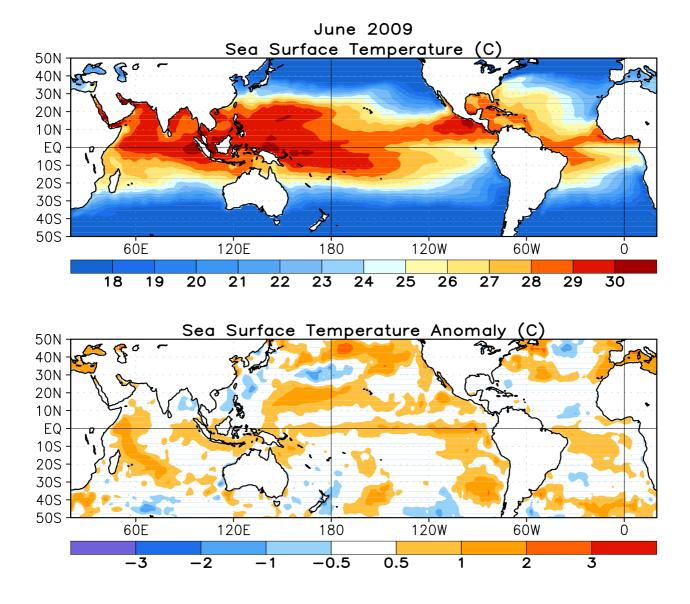


FIGURE T18. Mean (top) and anomalous (bottom) sea surface temperature (SST). Anomalies are departures from the 1971-2000 base period monthly means (Smith and Reynolds 1998, *J. Climate*, **11**, 3320-3323).

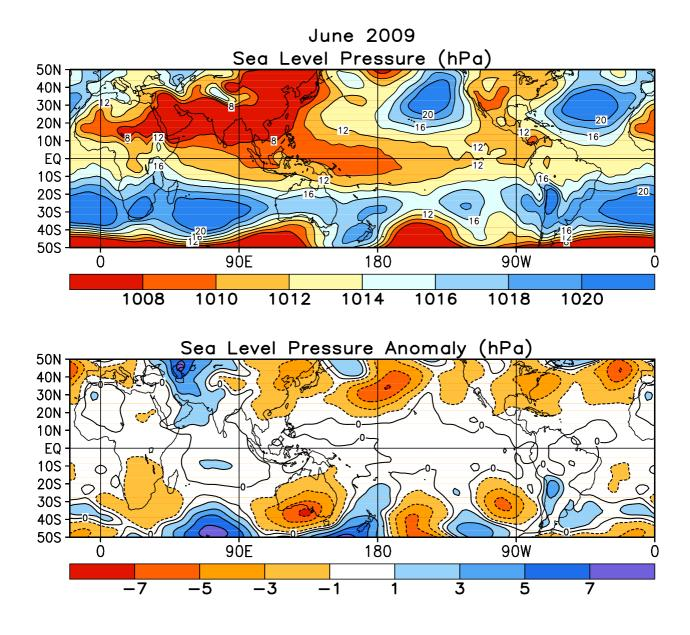


FIGURE T19. Mean (top) and anomalous (bottom) sea level pressure (SLP) (CDAS/Reanalysis). In top panel, 1000 hPa has been subtracted from contour labels, contour interval is 2 hPa, and values below 1000 hPa are indicated by dashed contours. In bottom panel, anomaly contour interval is 1 hPa and negative anomalies are indicated by dashed contours. Anomalies are departures from the 1979-1995 base period monthly means.

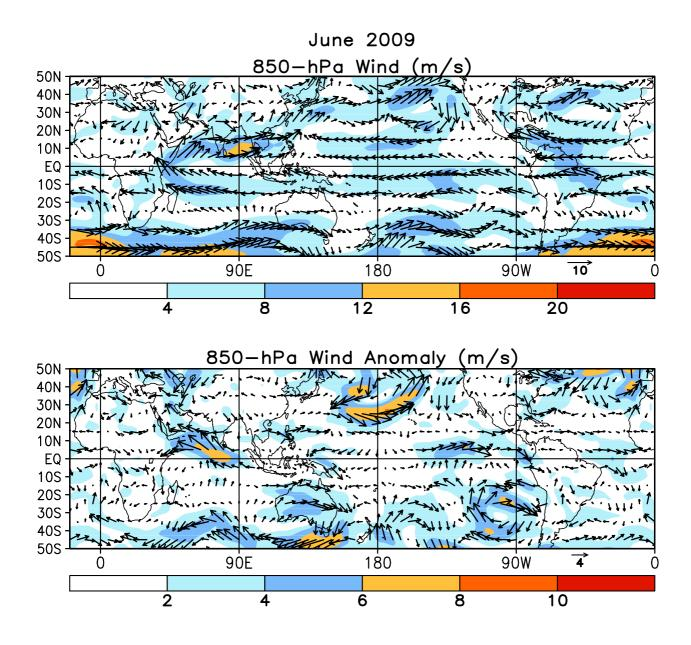


FIGURE T20. Mean (top) and anomalous (bottom) 850-hPa vector wind (CDAS/Reanaysis) for JUN 2009. Contour interval for isotachs is 4 ms⁻¹ (top) and 2 ms⁻¹ (bottom). Anomalies are departures from the 1979–95 base period monthly means.

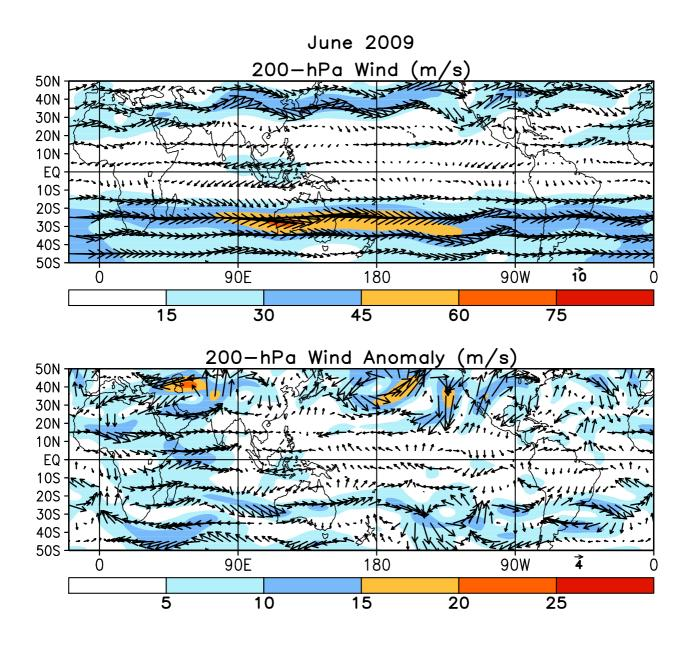


FIGURE T21. Mean (top) and anomalous (bottom) 200-hPa vector wind (CDAS/Reanalysis) for JUN 2009. Contour interval for isotachs is 15 ms⁻¹ (top) and 5 ms⁻¹ (bottom). Anomalies are departures from 1979–95 base period monthly means.

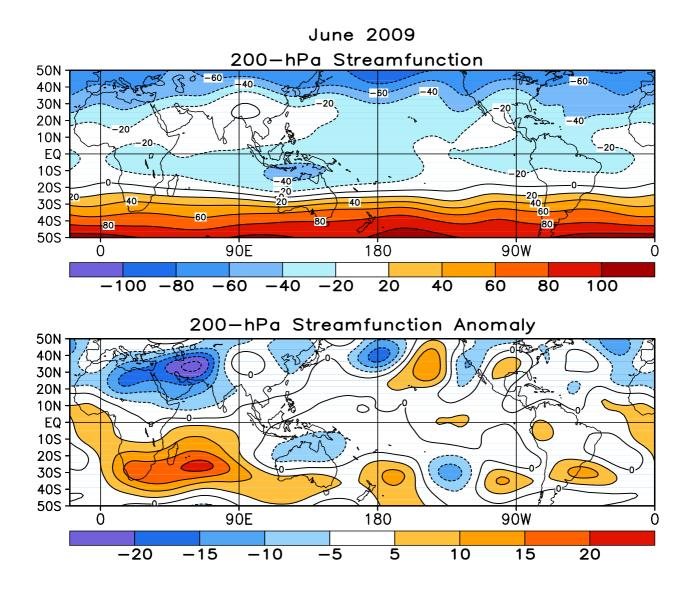


FIGURE T22. Mean (top) and anomalous (bottom) 200-hPa streamfunction (CDAS/Reanalysis). Contour interval is 20 x 10⁶ m²s⁻¹ (top) and 5 x 10⁶ m²s⁻¹ (bottom). Negative (positive) values are indicated by dashed (solid) lines. The non-divergent component of the flow is directed along the contours with speed proportional to the gradient. Thus, high (low) stream function corresponds to high (low) geopotential height in the Northern Hemisphere and to low (high) geopotential height in the Southern Hemisphere. Anomalies are departures from the 1979-1995 base period monthly means.

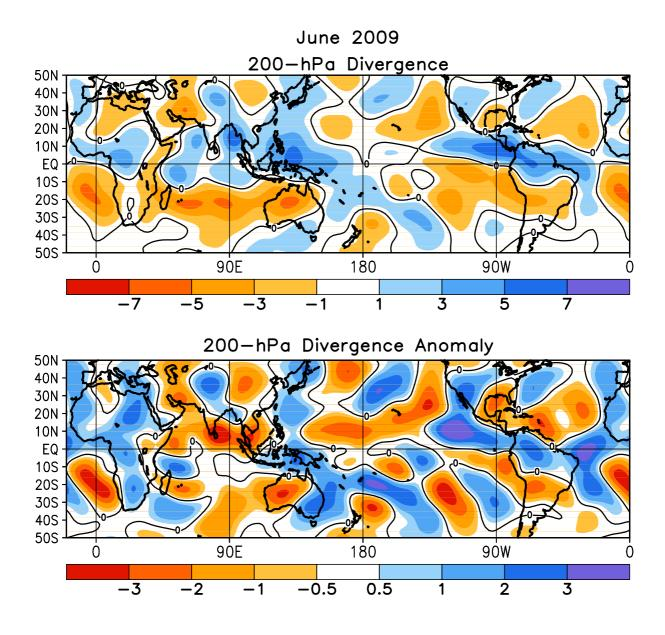


FIGURE T23. Mean (top) and anomalous (bottom) 200-hPa divergence (CDAS/Reanalysis). Divergence and anomalous divergence are shaded blue. Convergence and anomalous convergence are shaded orange. Anomalies are departures from the 1979-1995 base period monthly means.

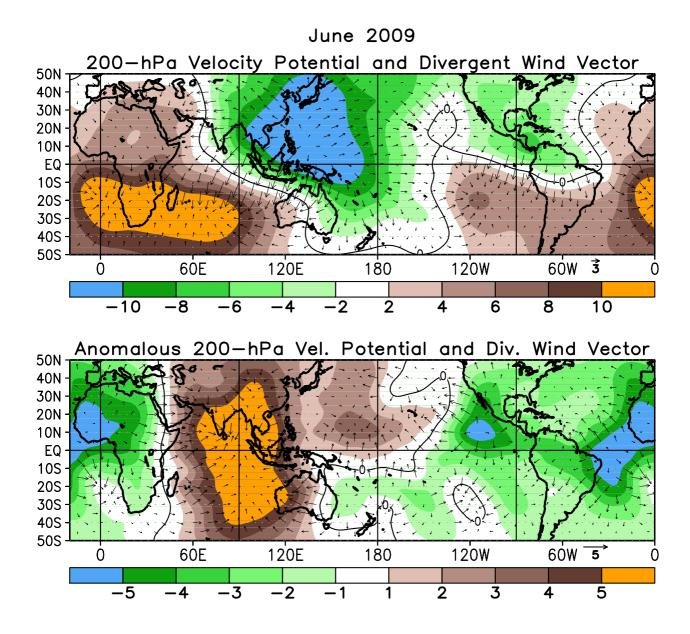


FIGURE T24. Mean (top) and anomalous (bottom) 200-hPa velocity potential (10⁶m²s) and divergent wind (CDAS/ Reanalysis). Anomalies are departures from the 1979-1995 base period monthly means.

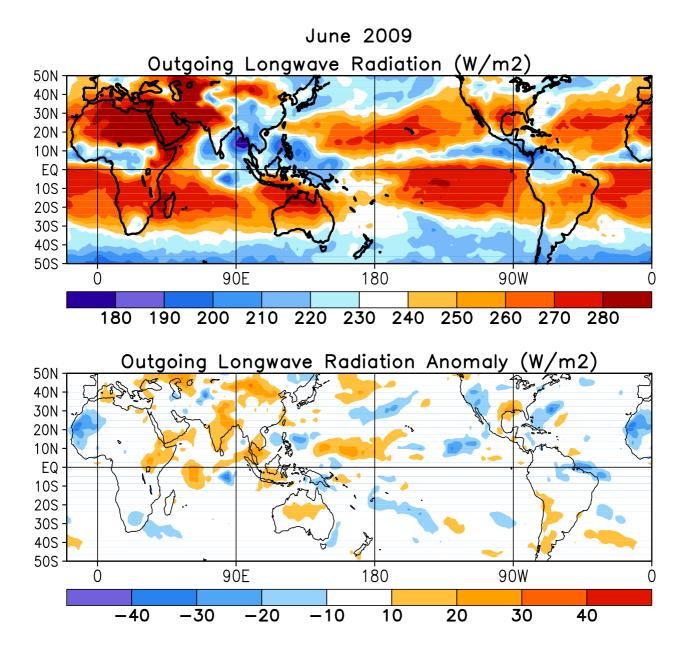


FIGURE T25. Mean (top) and anomalous (bottom) outgoing longwave radiation for JUN 2009 (NOAA 18 AVHRR IR window channel measurements by NESDIS/ORA). OLR contour interval is 20 Wm⁻² with values greater than 280 Wm⁻² indicated by dashed contours. Anomaly contour interval is 15 Wm⁻² with positive values indicated by dashed contours and light shading. Anomalies are departures from the 1979–95 base period monthly means.

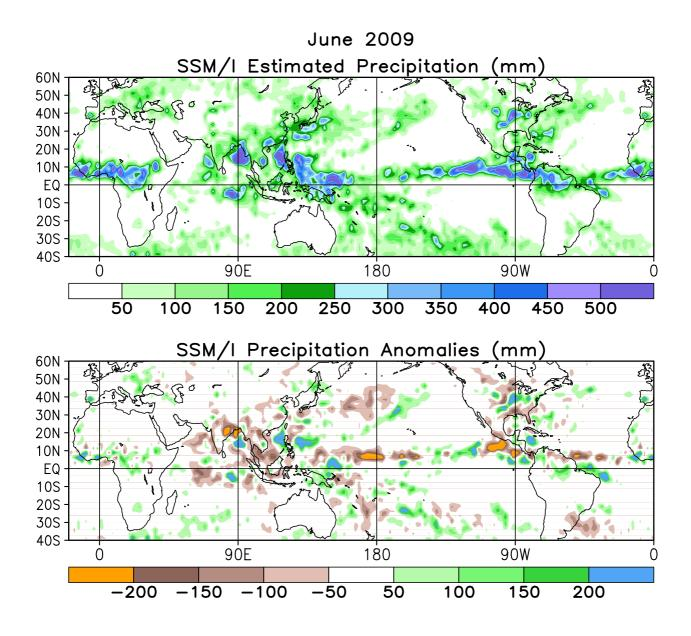


FIGURE T26. Estimated total (top) and anomalous (bottom) rainfall (mm) based on the Special Sensor Microwave/ Imager (SSM/I) precipitation index (Ferraro 1997, *J. Geophys. Res.*, **102**, 16715-16735). Anomalies are computed from the 1987-2006 base period monthly means. Anomalies have been smoothed for display purposes.

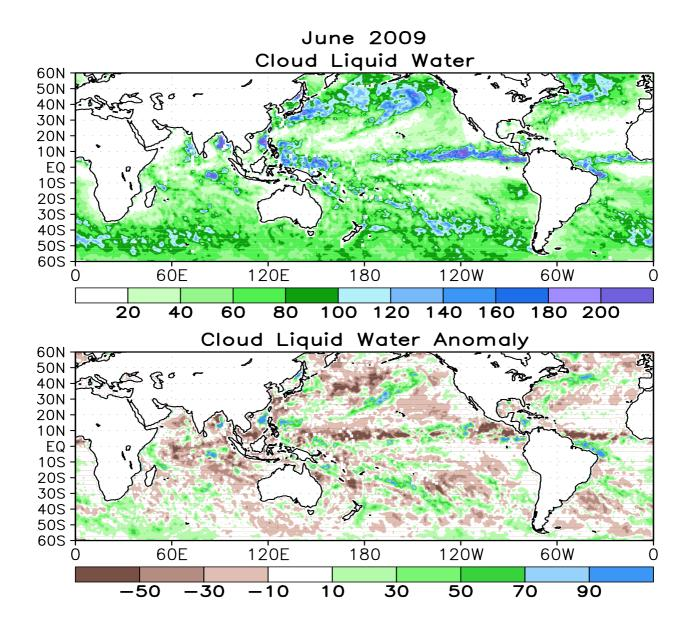


FIGURE T27. Mean (top) and anomalous (bottom) cloud liquid water (g m⁻²) based on the Special Sensor Microwave/ Imager (SSM/I) (Weng et al 1997: *J. Climate*, **10**, 1086-1098). Anomalies are calculated from the 1987-2006 base period means.

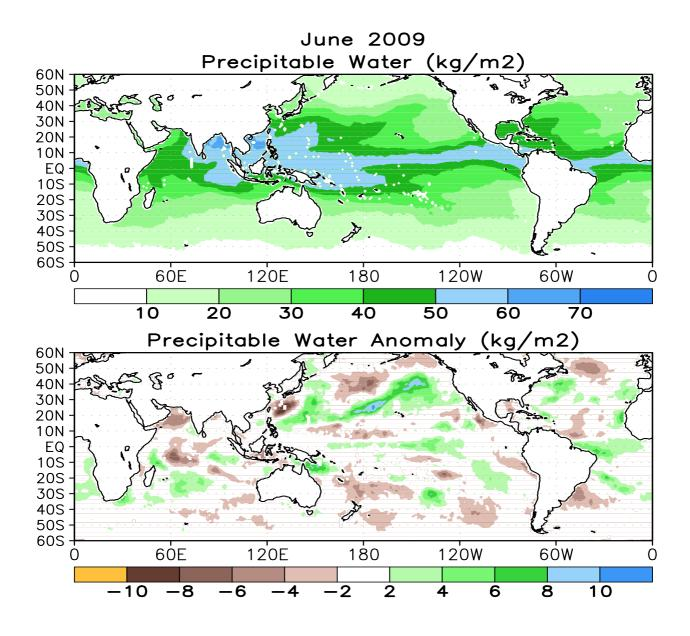


FIGURE T28. Mean (top) and anomalous (bottom) vertically integrated water vapor or precipitable water (kg m⁻²) based on the Special Sensor Microwave/Imager (SSM/I) (Ferraro et. al, 1996: *Bull. Amer. Meteor. Soc.*, **77**, 891-905). Anomalies are calculated from the 1987-2006 base period means.

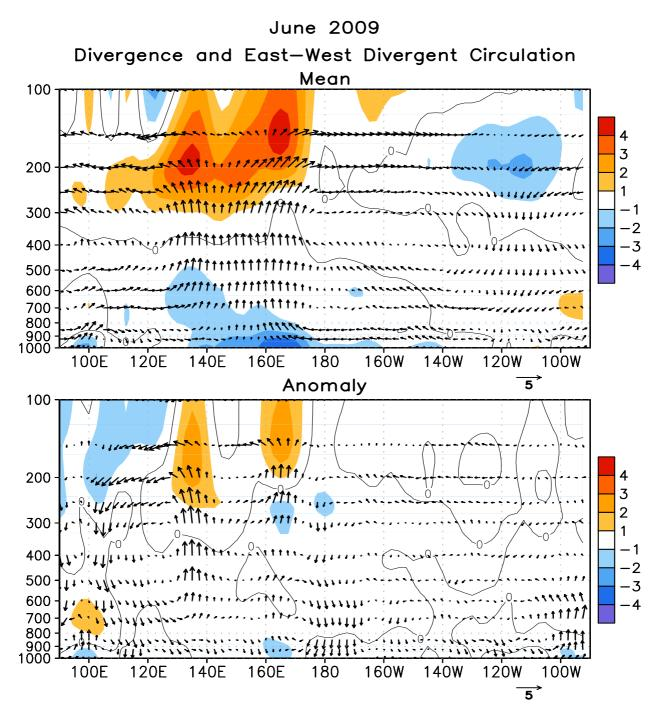


FIGURE T29. Pressure-longitude section (100E-80W) of the mean (top) and anomalous (bottom) divergence (contour interval is 1 x 10⁻⁶ s⁻¹) and divergent circulation averaged between 5N-5S. The divergent circulation is represented by vectors of combined pressure vertical velocity and the divergent component of the zonal wind. Red shading and solid contours denote divergence (top) and anomalous divergence (bottom). Blue shading and dashed contours denote convergence (top) and anomalous convergence (bottom). Anomalies are departures from the 1979-1995 base period monthly means.

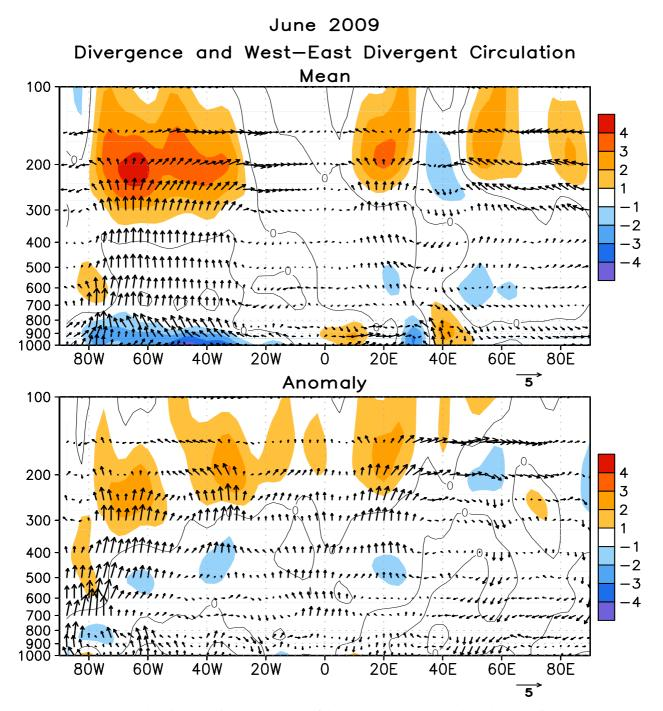


FIGURE T30. Pressure-longitude section (80W-100E) of the mean (top) and anomalous (bottom) divergence (contour interval is 1 x 10⁻⁶ s⁻¹) and divergent circulation averaged between 5N-5S. The divergent circulation is represented by vectors of combined pressure vertical velocity and the divergent component of the zonal wind. Red shading and solid contours denote divergence (top) and anomalous divergence (bottom). Blue shading and dashed contours denote convergence (top) and anomalous convergence (bottom). Anomalies are departures from the 1979-1995 base period monthly means.

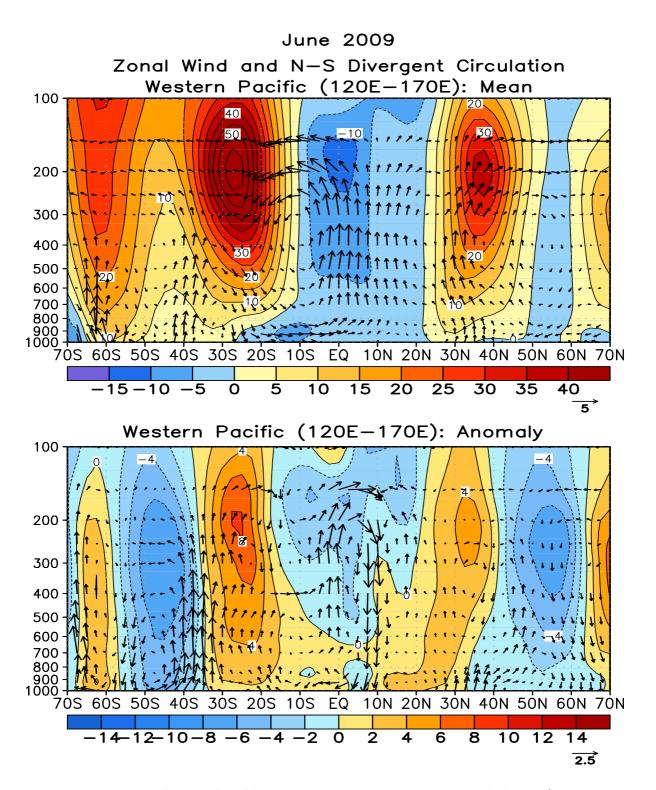


FIGURE T31. Pressure-latitude section of the mean (top) and anomalous (bottom) zonal wind (m s⁻¹) and divergent circulation averaged over the west Pacific sector (120E-170E). The divergent circulation is represented by vectors of combined pressure vertical velocity and the divergent component of the meridional wind. Red shading and solid contours denote a westerly (top) or anomalous westerly (bottom) zonal wind. Blue shading and dashed contours denote an easterly (top) or anomalous easterly (bottom) zonal wind. Anomalies are departures from the 1979-1995 base period monthly means.

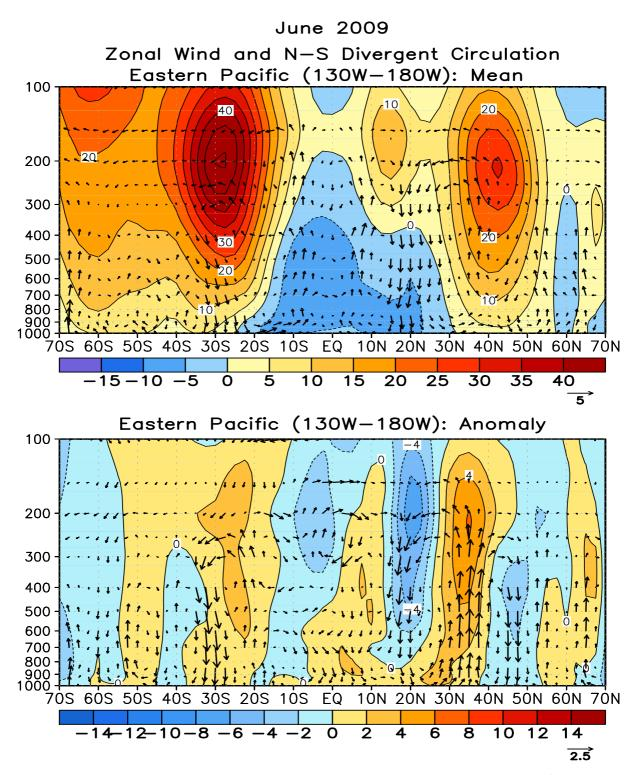
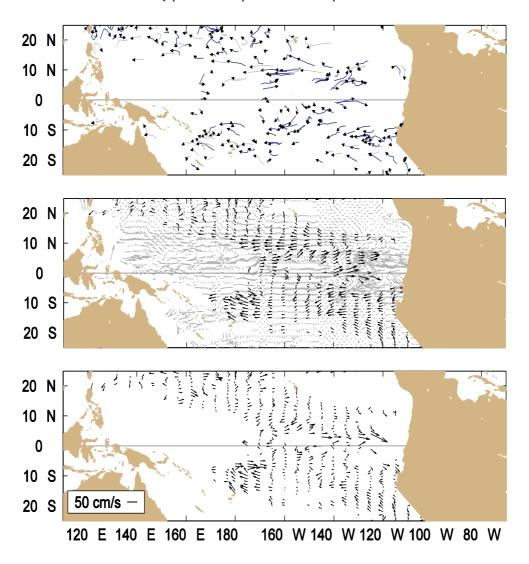
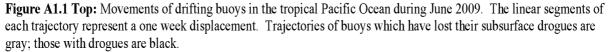


FIGURE T32. Pressure-latitude section of the mean (top) and anomalous (bottom) zonal wind (m s⁻¹) and divergent circulation averaged over the central Pacific sector (130W-180W). The divergent circulation is represented by vectors of combined pressure vertical velocity and the divergent component of the meridional wind. Red shading and solid contours denote a westerly (top) or anomalous westerly (bottom) zonal wind. Blue shading and dashed contours denote an easterly (top) or anomalous easterly (bottom) zonal wind. Anomalies are departures from the 1979-1995 base period monthly means.

Tropical Pacific Drifting Buoys R. Lumpkin/M. Pazos, AOML, Miami

During June 2009, 355 satellite-tracked surface drifting buoys, 72% with subsurface drogues attached for measuring mixed layer currents, were reporting from the tropical Pacific. North of 10S, eastward anomalies have intensified since last month, with magnitudes of 10-20 cm/s now seen across the basin. In the narrow band of the NECC at 10N, weak westward anomalies were measured by several drifters. From 10-22S, westward anomalies of O(10 cm/s) were common across the basin. Most drifters away from the northwest corner of the region measured SST at or above normal June values, with anomalies of +0.5 to +1.5C very common. Warm anomalies were especially prevalent in the southeast tropical Pacific. Cold anomalies (-0.5C to -3.0C) were measured by many drifters in the northwest, north of 20N and west of the dateline. These SST anomaly patterns have persisted over the previous several months.





Middle: Monthly mean currents calculated from all buoys 1993-2002 (gray), and currents measured by the drogued buoys this month (black) smoothed by an optimal filter.

Bottom: Anomalies from the climatological monthly mean currents for this month.

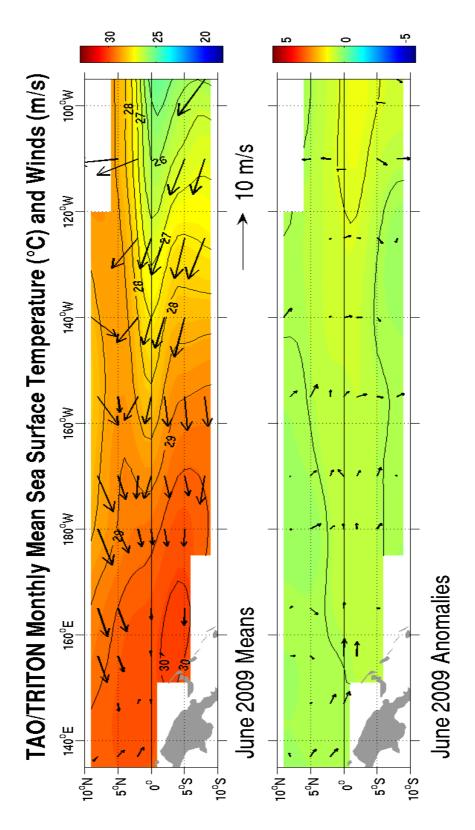
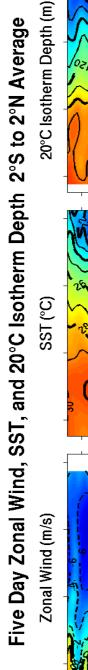
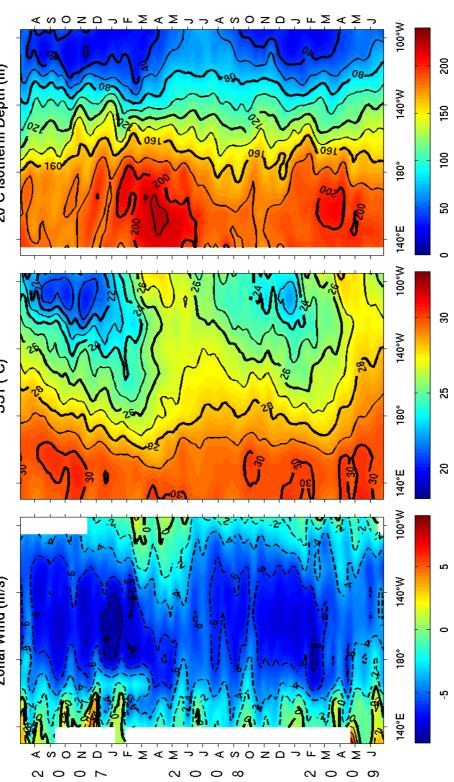
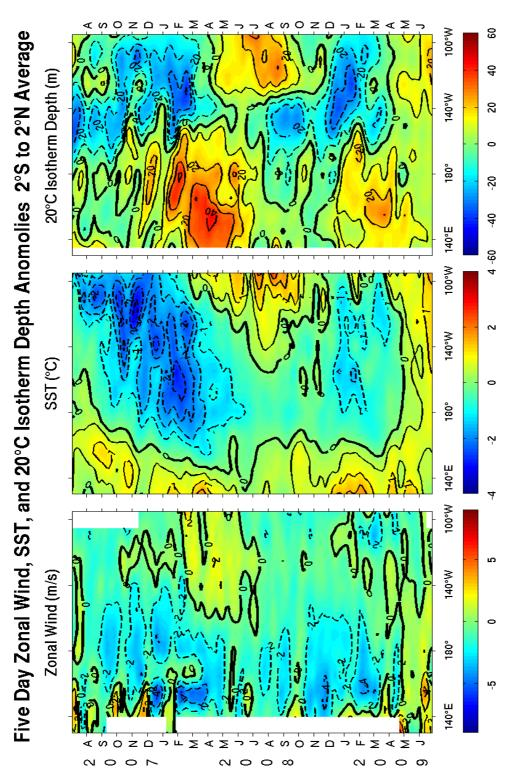


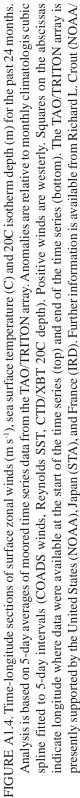
FIGURE A1.2. Wind Vectors and sea surface temperature (SSTs) from the TAO/TRITON mooring array. Top panel shows monthly means; bottom panel shows monthly anomalies from the COADS wind climatology and Reynolds SST climatology (1971-2000). The TAO/TRITON array is presently supported by the United States (NOAA), Japan (STA), and France (IRD). Further information is available from Richard L. Crout (NOAA/NDBC).

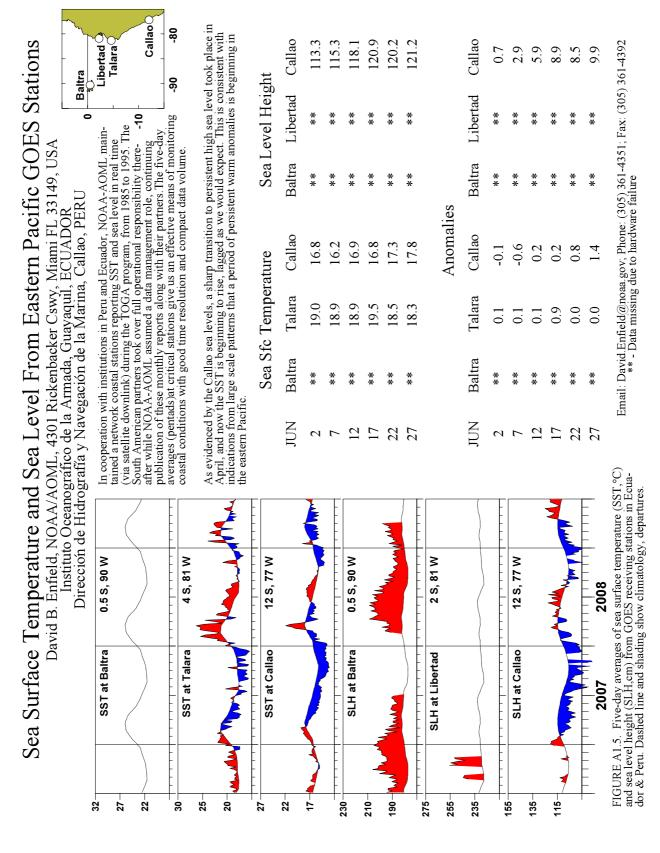


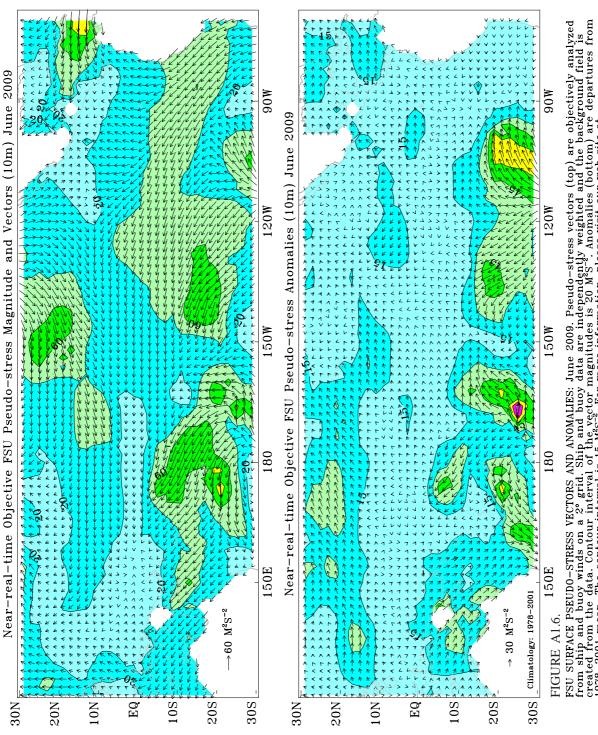


Analysis is based on 5-day averages of moored time series data from the TAO/TRITON array. Positive winds are westerly. Squares on the abscissas indicate longitude where data were available at the start of the time series (top) and end of the time series (bottom). The TAO/TRITON array is presently supported by the United States (NOAA), Japan (STA), and France (IRD). Further information is available from Richard L. Crout (NOAA/ FIGURE A1.3. Time-longitude sections of surface zonal winds (m s⁻¹), sea surface temperature (C) and 20C isotherm depth (m) for the past 24 months. NDBC)

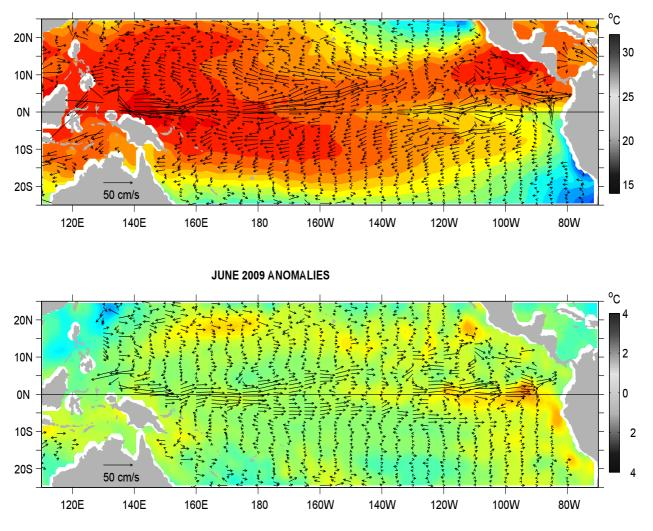






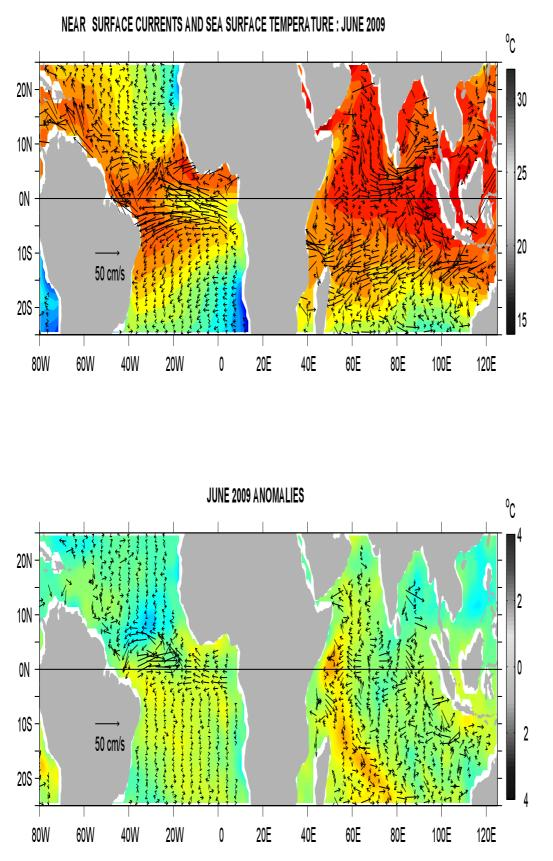






NEAR SURFACE CURRENTS AND SEA SURFACE TEMPERATURE : JUNE 2009

FIGURE A1.7. Ocean Surface Current Analysis-Real-time (OSCAR) for JUN 2009 (Bonjean and Lagerloef 2002, J. Phys. Oceanogr., Vol. 32, No. 10, 2938-2954; Lagerloef et al. 1999, JGR-Oceans, 104, 23313-23326). (top) Total velocity. Satellite data included JUN 2009 Jason sea level anomalies and QuickScat winds. (bottom) Velocity anomalies. The subtracted climatology was based on SSM/I and QuickScat winds and Topex/Poseidon and Jason from 1993-2003. See also http://www.oscar.noaa.gov.





Forecast Forum

The canonical correlation analysis (CCA) forecast of SST in the central Pacific (Barnett et al. 1988, *Science*, **241**, 192196; Barnston and Ropelewski 1992, *J. Climate*, **5**, 13161345), is shown in **Figs. F1 and F2.** This forecast is produced routinely by the Prediction Branch of the Climate Prediction Center. The predictions from the National Centers for Environmental Prediction (NCEP) Coupled Forecast System Model (CFS03) are presented in **Figs. F3 and F4a, F4b**. Predictions from the Markov model (Xue, et al. 2000: *J. Climate*, **13**, 849871) are shown in **Figs. F5 and F6**. Predictions from the latest version of the LDEO model (Chen et al. 2000: *Geophys. Res. Let.*, **27**, 25852587) are shown in **Figs. F7 and F8**. Predictions using linear inverse modeling (Penland and Magorian 1993: *J. Climate*, **6**, 10671076) are shown in **Figs. F9 and F10**. Predictions from the Scripps / Max Planck Institute (MPI) hybrid coupled model (Barnett et al. 1993: *J. Climate*, **6**, 15451566) are shown in **Fig. F11**. Predictions from the ENSOCLIPER statistical model (Knaff and Landsea 1997, *Wea. Forecasting*, **12**, 633652) are shown in **Fig. F12**. Niño 3.4 predictions are summarized in **Fig. F13**, provided by the Forecasting and Prediction Research Group of the IRI.

The CPC and the contributors to the **Forecast Forum** caution potential users of this predictive information that they can expect only modest skill.

ENSO Alert System Status

El Niño Advisory

Outlook

El Niño conditions will continue to develop and are expected to last through the Northern Hemisphere Winter 2009-2010.

Discussion

During June 2009, conditions across the equatorial Pacific Ocean transitioned from ENSO-neutral to El Niño conditions. Sea surface temperature (SST) anomalies continued to increase, with the latest monthly departures exceeding +0.5°C across the equatorial Pacific (**Fig. T18**). All of the SST indices increased during June and now range from +0.6°C to +0.7°C (**Table T2**). Subsurface oceanic heat content anomalies (average temperatures in the upper 300m of the ocean) also increased as the thermocline continued to deepen (**Fig. T17**). Consistent with the oceanic evolution, the low-level equatorial trade winds were weaker-than-average across the eastern Pacific basin (**Fig. T20**), and convection became increasingly suppressed over Indonesia (**Fig. T25**). This coupling of the oceanic and atmospheric anomalies indicates the development of El Niño conditions.

Model forecasts of SST anomalies for the Niño-3.4 region (**Figs. F1-F13**) reflect a growing consensus for the continued development of El Niño ($+0.5^{\circ}$ C or greater in the Niño-3.4 region). However, the spread of the models indicates disagreement over the eventual strength of El Niño ($+0.5^{\circ}$ C to $+2.0^{\circ}$ C). Current conditions and recent trends favor the continued development of a weak-to-moderate strength El Niño into the Northern Hemisphere Fall 2009, with further strengthening possible thereafter.

Weekly updates of oceanic and atmospheric conditions are available on the Climate Prediction Center homepage (<u>El Niño/La Niña Current Conditions and Expert Discussions</u>).

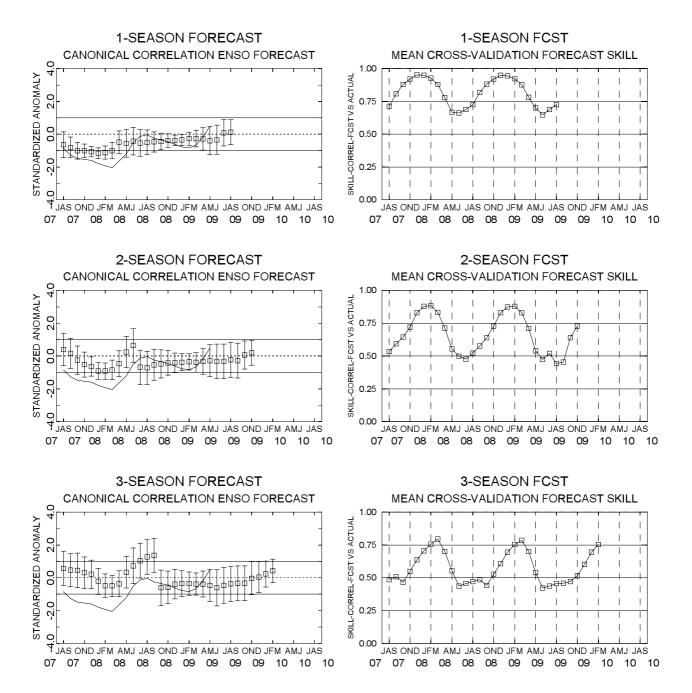


FIGURE F1. Canonical correlation analysis (CCA) sea surface temperature (SST) anomaly prediction for the central Pacific (5°N to 5°S, 120°W to 170°W (Barnston and Ropelewski, 1992, *J. Climate*, **5**, 1316-1345). The three plots on the left hand side are, from top to bottom, the 1-season, 2-season, and 3-season lead forecasts. The solid line in each forecast represents the observed SST standardized anomaly through the latest month. The small squares at the mid-points of the forecast bars represent the real-time CCA predictions based on the anomalies of quasi-global sea level pressure and on the anomalies of tropical Pacific SST, depth of the 20°C isotherm and sea level height over the prior four seasons. The vertical lines represent the one standard deviation error bars for the predictions based on past performance. The three plots on the right side are skills, corresponding to the predicted and observed SST. The skills are derived from cross-correlation tests from 1956 to present. These skills show a clear annual cycle and are inversely proportional to the length of the error bars depicted in the forecast time series.

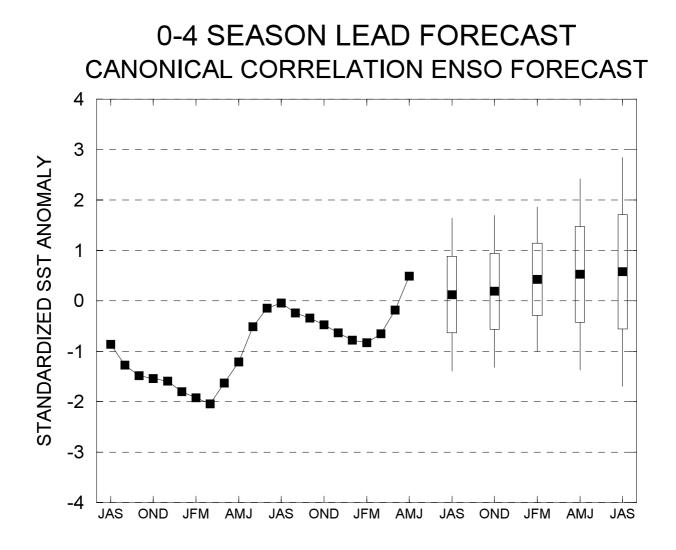


FIGURE F2. Canonical Correlation Analysis (CCA) forecasts of sea-surface temperature anomalies for the Nino 3.4 region (5N-5S, 120W-170W) for the upcoming five consecutive 3-month periods. Forecasts are expressed as standardized SST anomalies. The CCA predictions are based on anomaly patterns of SST, depth of the 20C isotherm, sea level height, and sea level pressure. Small squares at the midpoints of the vertical forecast bars represent the CCA predictions, and the bars show the one (thick) and two (thin) standard deviation errors. The solid continuous line represents the observed standardized three-month mean SST anomaly in the Nino 3.4 region up to the most recently available data.

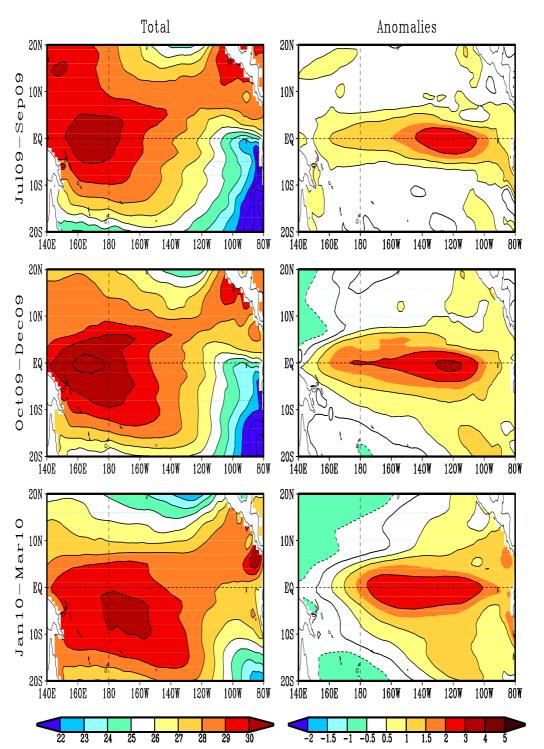


FIGURE F3. Predicted 3-month average sea surface temperature (left) and anomalies (right) from the NCEP Coupled Forecast System Model (CFS03). The forecasts consist of 40 forecast members. Contour interval is 1°C, with additional contours for 0.5°C and -0.5°C. Negative anomalies are indicated by dashed contours.

Last update: Fri Jul 3 2009 Initial conditions: 22Jun2009-01Jul2009

Last update: Fri Jul 3 2009 Initial conditions: 22Jun2009-01Jul2009

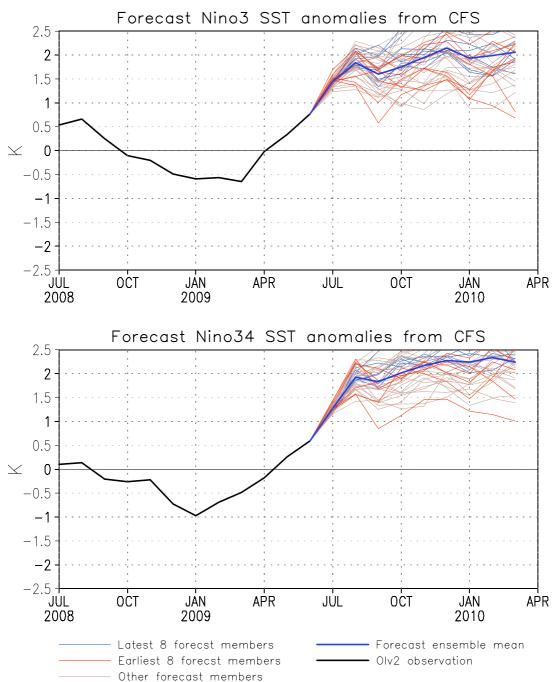


FIGURE F4. Predicted and observed sea surface temperature (SST) anomalies for the Nino 3 (top) and Nino 3.4 (bottom) regions from the NCEP Coupled Forecast System Model (CFS03). The forecasts consist of 40 forecast members. The ensemble mean of all 40 forecast members is shown by the blue line, individual members are shown by thin lines, and the observation is indicated by the black line. The Nino-3 region spans the eastern equatorial Pacific between 5N-5S, 150W-90W. The Nno 3.4 region spans the east-central equatorial Pacific between 5N-5S, 170W-120W.

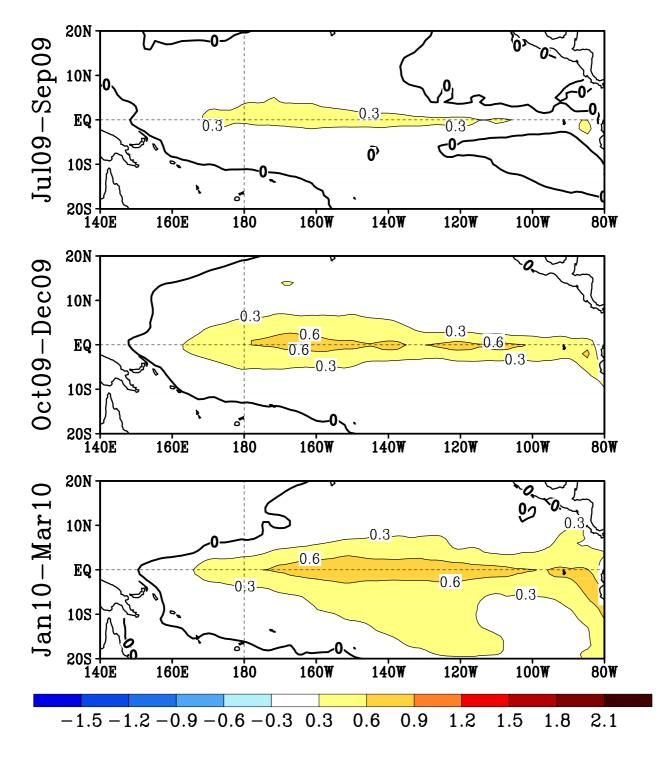
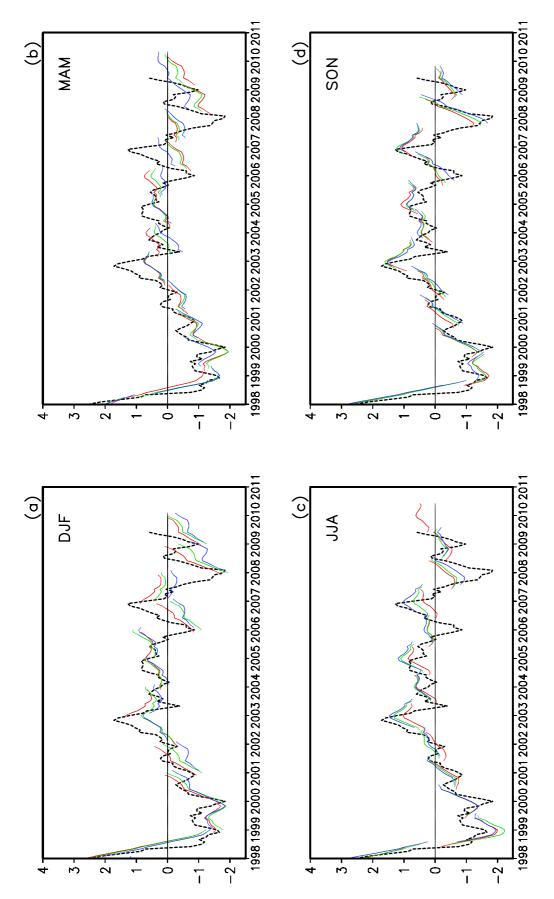
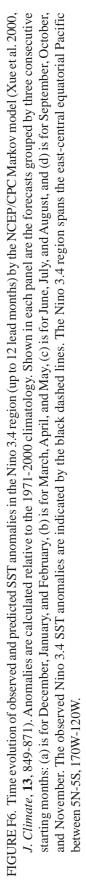
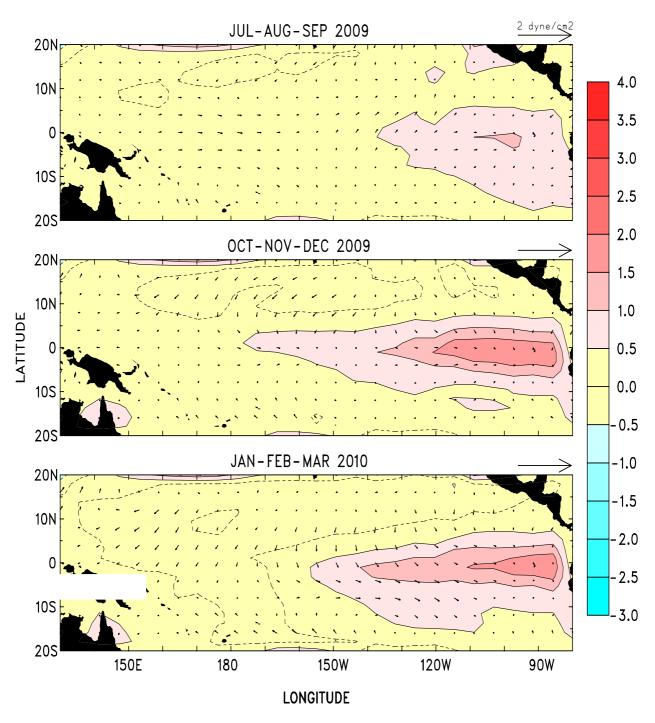


FIGURE F5. Predicted 3-month average sea surface temperature anomalies from the NCEP/CPC Markov model (Xue et al. 2000, *J. Climate*, **13**, 849-871). The forecast is initiated in JUN 2009. Contour interval is 0.3C and negative anomalies are indicated by dashed contours. Anomalies are calculated relative to the 1971-2000 climatology.







LDEO FORECASTS OF SST AND WIND STRESS ANOMALIES

FIGURE F7. Forecasts of the tropical Pacific Predicted SST (shading) and vector wind anomalies for the next 3 seasons based on the LDEO model. Each forecast represents an ensemble average of 3 sets of predictions initialized during the last three consecutive months (see Figure F8).

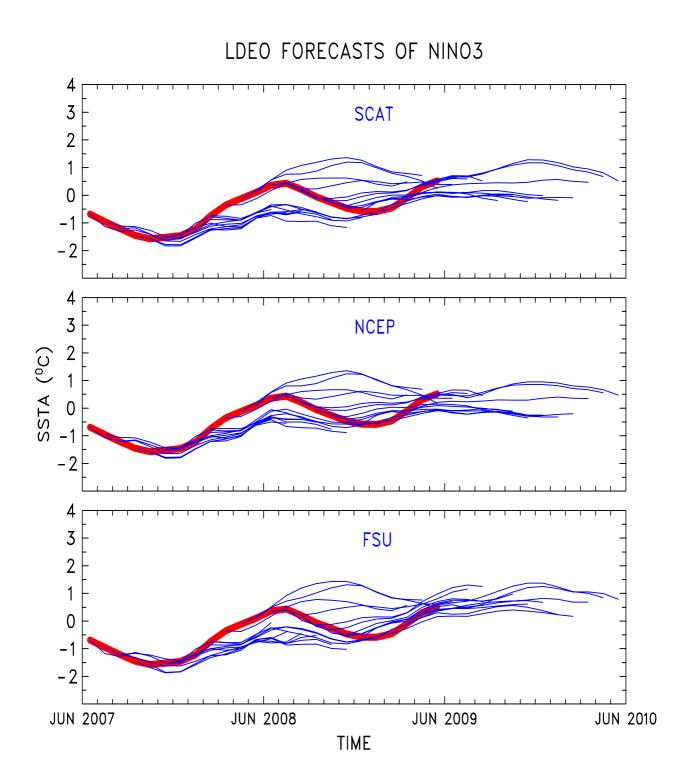


FIGURE F8. LDEO forecasts of SST anomalies for the Nino 3 region using wind stresses obtained from (top) QuikSCAT, (middle) NCEP, and (bottom) Florida State Univ. (FSU), along with SSTs (obtained from NCEP), and sea surface height data (obtained from TOPEX/POSEIDON) data. Each thin blue line represents a 12-month forecast, initialized one month apart for the past 24 months. Observed SST anomalies are indicated by the thick red line. The Nino-3 region spans the eastern equatorial Pacific between 5N-5S, 150W-90W.

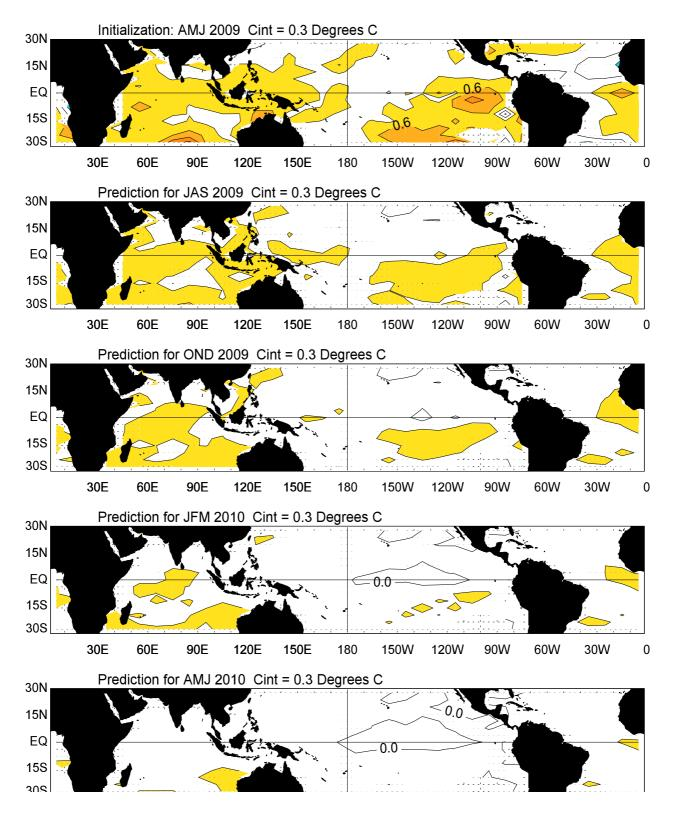


FIGURE F9. Forecast of tropical SST anomalies from the Linear Inverse Modeling technique of Penland and Magorian (1993: *J. Climate*, **6**, 1067-1076). The contour interval is 0.3C. Anomalies are calculated relative to the 1951-2000 climatology and are projected onto 20 leading EOFs.

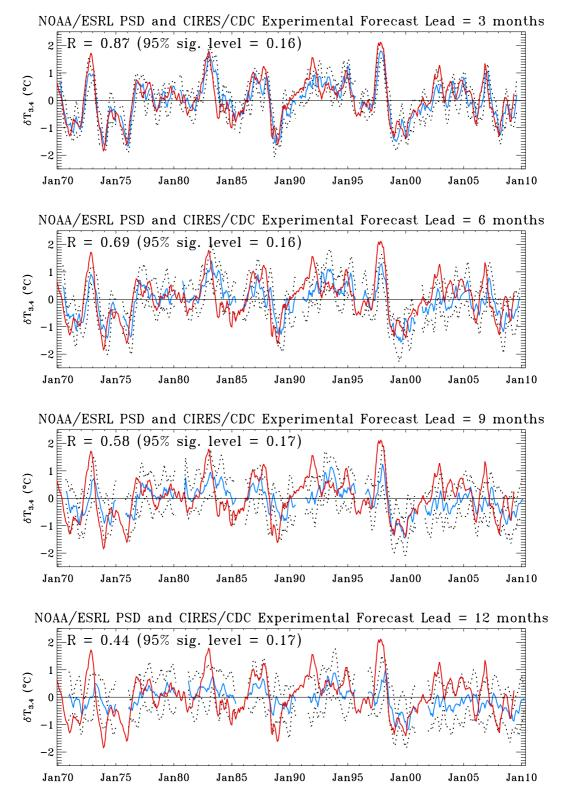


FIGURE F10. Predictions of SST anomalies in the Nino3.4 region (blue line) for leads of three months (top) to 12 months (bottom), from the Linear Inverse Modeling technique of Penland and Magorian (1993: *J. Climate*, **6**, 1067-1076). Observed SST anomalies are indicated by the red line. Anomalies are calculated relative to the 1951-2000 climatology and are projected onto 20 leading EOFs. The Nino 3.4 region spans the east-central equatorial Pacific between 5N-5S, 170W-120W.

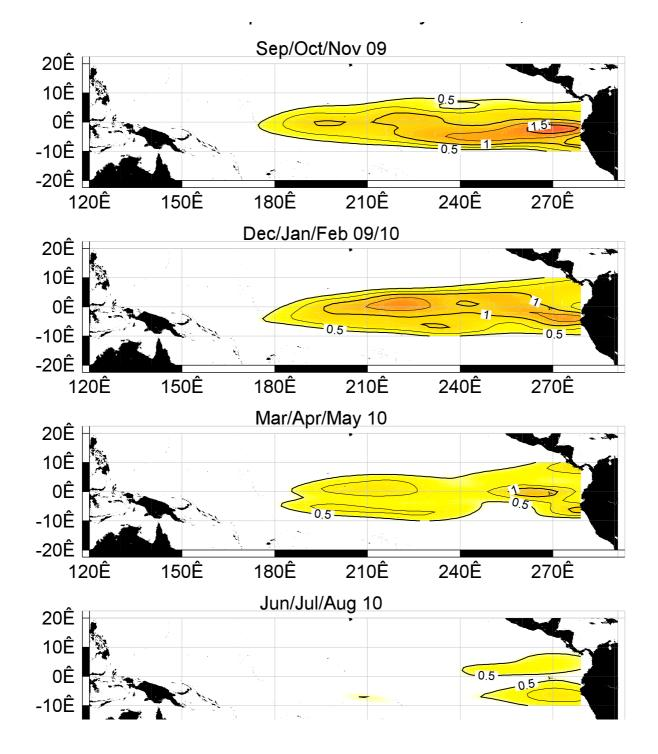


FIGURE F11. SST anomaly forecast for the equatorial Pacific from the Hybrid Coupled Model (HCM) developed by the Scripps Institution of Oceanography and the Max-Plank Institut fuer Meteorlogie.

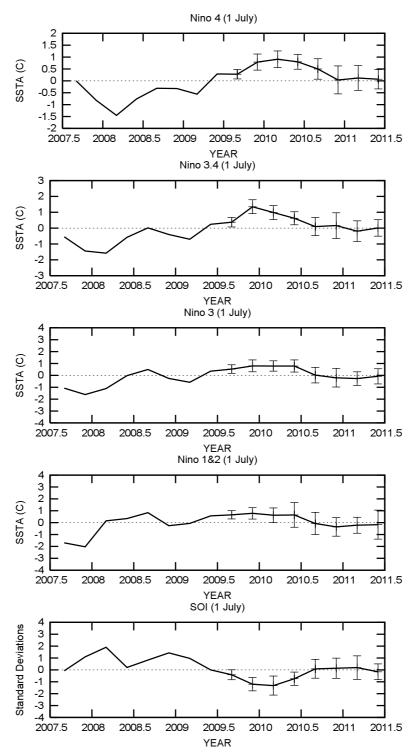


FIGURE F12. ENSO-CLIPER statistical model forecasts of three-month average sea surface temperature anomalies (green lines, deg. C) in (top panel) the Nino 4 region (5N-5S, 160E-150W), (second panel) the Nino 3.4 region (5N-5S, 170W-120W), (third panel) the Nino 3 region (5N-5S, 150W-90W), and (fourth panel) the Nino 1+2 region (0-10S, 90W-80W) (Knaff and Landsea 1997, *Wea. Forecasting*, **12**, 633-652). Bottom panel shows predictions of the three-month standardized Southern Oscillation Index (SOI, green line). Horizontal bars on green line indicate the adjusted root mean square error (RMSE). The Observed three-month average values are indicated by the thick blue line. SST anomalies are departures from the 1971-2000 base period means, and the SOI is calculated from the 1951-1980 base period means.

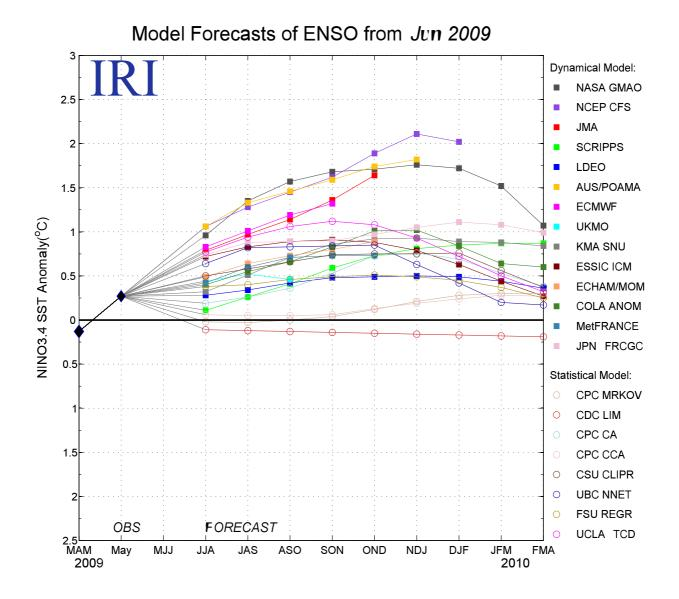


FIGURE F13. Time series of predicted sea surface temperature anomalies for the Nino 3.4 region (deg. C) from various dynamical and statistical models for nine overlapping 3-month periods. The Nino 3.4 region spans the east-central equatorial Pacific between 5N-5S, 170W-120W. Figure provided by the International Research Institute (IRI).

Extratropical Highlights – June 2009

1. Northern Hemisphere

The 500-hPa height field during June 2009 featured large areas of negative anomalies in the middle latitudes and generally positive anomalies at high latitudes (**Fig. E9**). This pattern was associated with large amplitude troughs over the central North Pacific, the western U.S., the eastern North Atlantic, and Mongolia, and with ridges over the high latitudes of the North Atlantic, near the Caspian Sea, and over eastern Siberia.

The 200-hPa streamfunction field indicated near average conditions in the subtropics across the eastern half of the Pacific Ocean, in association with the demise of La Niña and the onset of weak El Niño conditions (**Fig. T22**). Also, the combination of negative streamfunction anomalies from north-central Africa to Pakistan and positive anomalies across the subtropical Indian Ocean reflected weaker subtropical ridges that were contracted equatorward in both hemispheres.

The main temperature signals during June included above average temperatures in the southeastern U.S., southern Europe, and China, and below average temperatures in the northern Plains States and central Canada (**Fig. E1**). The main precipitation signals included above average totals across the central U.S., eastern Europe, and Mongolia, and below average totals in southwestern Russia, India, and southeastern Asia (**Fig. E3**).

a. North Pacific/ North America

This is the first time in almost a year that no La Niña signal was evident in the NH extratropical circulation. During June, strong 500-hPa troughs were evident over the central North Pacific, the south-western U.S., and the extreme western North Atlantic (**Fig. E9**). Between the trough axes, enhanced anticyclonic curvature was evident in the Gulf of Alaska and over the southern U.S. (**Fig. T22**). Also, a confluent flow configuration was present in the Intermountain region in response to the combination of an anomalous zonal flow over the northern U.S. and the trough in the southwest.

This overall circulation contributed to above average precipitation from Oregon to the northeastern U.S., with the most significant surpluses observed in the Inter-Mountain, Great Plains, Mid-Atlantic, and Northeast regions of the U.S. (**Figs. E5, E6**). In contrast, anomalously dry (and warm) conditions were observed in the Gulf Coast region. Rainfall totals from eastern Texas to western Mississippi were less than 25% of normal and in the lowest 10th percentile of occurrences.

b. North Atlantic and Europe

The 500-hPa circulation during June featured a dipole pattern of 500-hPa height anomalies over the North Atlantic, with above average heights in the north and below average heights in the middle latitudes (**Fig. E9**). This pattern reflected the negative phases of both the NAO and EA teleconnection pattern (**Table E1**). The trough over the eastern North Atlantic Ocean, combined with a strong ridge over the Caspian Sea contributed to above average temperatures across southern Europe and portions of the Middle East, with some areas recording values in the upper 90th percentile of occurrences (**Fig. E1**).

c. India

The circulation during June featured a reduced strength of the Indian monsoon ridge at 200-hPa, and a confinement of the subtropical ridge to central China (**Fig. T22**). This pattern was associated with a slow start to the Indian monsoon season, with area-averaged monsoon rainfall in the lowest 10th percentile of occurrences (**Fig. E4**).

2. Southern Hemisphere

The circulation during June reflected a zonal wave-2 pattern of 500-hPa height anomalies in the middle latitudes, and wave-1 pattern at high latitudes (**Fig. E15**). Aspects of this pattern included above average heights over the southern Indian Ocean, and below average heights over southern Australia and the east-central South Pacific.

In the subtropics, the 200-hPa streamfunction pattern featured positive anomalies from southern Africa to Australia, in association with a reduced strength of the subtropical ridge. Consistent with this pattern, anomalous upper-level westerly winds and above average rainfall extended across the subtropical Indian Ocean and southern Australia (**Fig. E3**).

TELECONNECTION INDICES

NORTH ATLANTIC NORTH PACIFIC

EURASIA

MONTH	NAO	EA	WP	EP-NP	ANA	HNT	EATL/ WRUS	SCAND	POLEUR
60 NN	-1.2	-1.0	-1.6	-0.1	7.0		0.7	-0.1	0.2
MAY 09	1.7	1.5	-1.2	1.6	9.0-		0.2	0.2	-0.8
APR 09	-0.2	<i>L</i> .0	-0.1	9.0	0.2		1.4	-0.2	1.8
MAR 09	0.6	6.0-	0.4	-1.0	-1.0		0.1	-0.7	-0.9
FEB 09	0.1	-0.5	2.2	0.6	6.0-	0.4	-0.8	9.0	-0.4
JAN 09	0.0	1.6	0.4	-0.3	9.0	1.9	-1.4	-0.1	0.3
DEC 08	-0.3	-0.6	1.1		-1.4	2.1	-1.5	0.1	-0.8
NOV 08	-0.3	-0.5	0.3	0.8	1.1		-1.0	-1.0	0.3
OCT 08	0.0	0.5	-0.1	-1.2	6.0		-1.3	-1.1	1.4
SEP 08	1.0	0.0	-0.6	-0.7	1.1		-0.9	1.1	-0.1
AUG 08	-1.2	0.6	-1.5	-1.1	0.9		-0.5	-0.6	1.1
JUL 08	-1.3	1.6	-0.6	-1.0	-0.1		0.2	1.1	-0.2
JUN 08	-1.4	1.0	-0.5	-0.6	-1.8		-0.3	-0.6	0.4

in Fig. E7). Pattern names and abbreviations are North Atlantic Oscillation (NAO); East Atlantic pattern (EA); West Pacific pattern (WP); East Pacific - North Pacific TABLE E1-Standardized amplitudes of selected Northern Hemisphere teleconnection patterns for the most recent thirteen months (computational procedures are described pattern (EP-NP); Pacific/North American pattern (PNA); Tropical/Northern Hemisphere pattern (TNH); East Atlantic/Western Russia pattern (EATL/WRUS-called Eurasia-2 pattern by Barnston and Livezey, 1987, Mon. Wea. Rev., 115, 1083-1126); Scandanavia pattern (SCAND-called Eurasia-1 pattern by Barnston and Livezey 1987); and Polar Eurasia pattern (POLEUR). No value is plotted for calendar months in which the pattern does not appear as a leading mode.

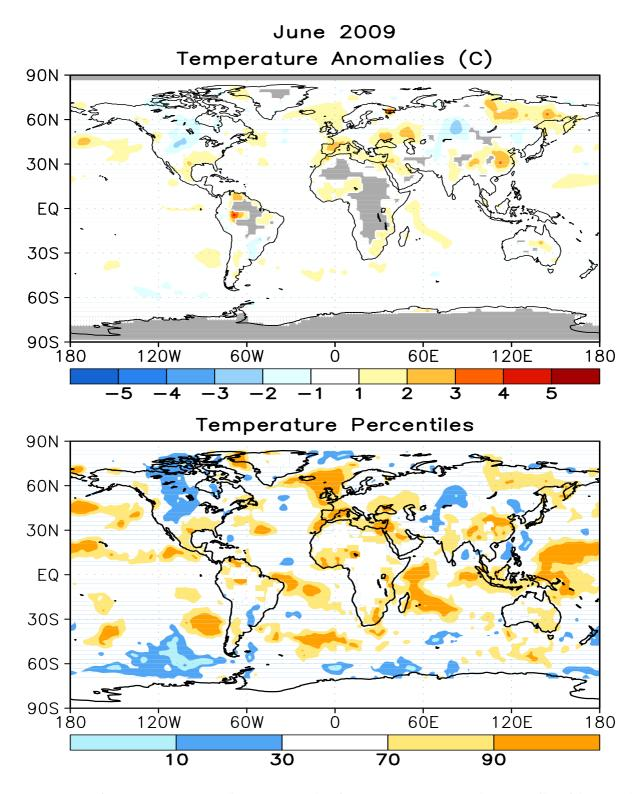


FIGURE E1. Surface temperature anomalies (°C, top) and surface temperature expressed as percentiles of the normal (Gaussian) distribution fit to the 1971–2000 base period data (bottom) for JUN 2009. Analysis is based on station data over land and on SST data over the oceans (top). Anomalies for station data are departures from the 1971–2000 base period means, while SST anomalies are departures from the 1971–2000 adjusted OI climatology. (Smith and Reynolds 1998, *J. Climate*, **11**, 3320-3323). Regions with insufficient data for analysis in both figures are indicated by shading in the top figure only.

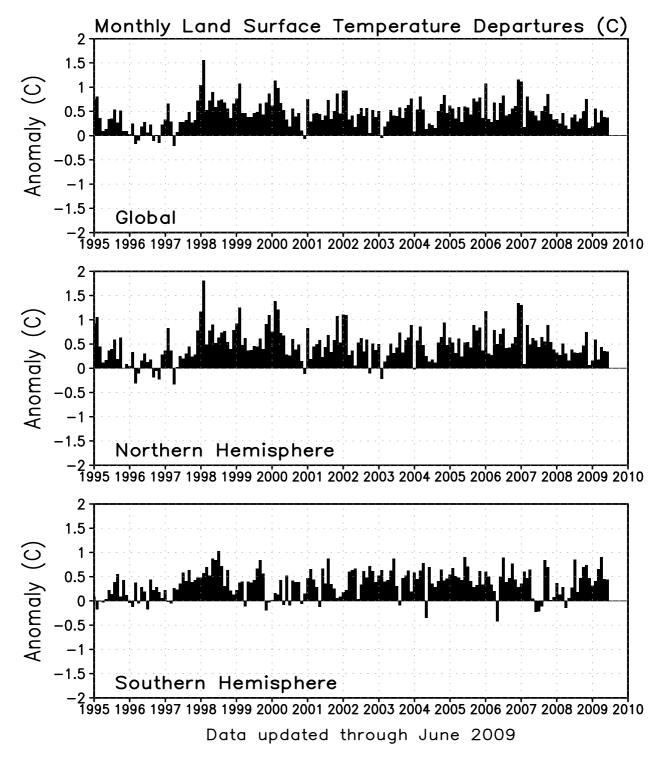


FIGURE E2. Monthly global (top), Northern Hemisphere (middle), and Southern Hemisphere (bottom) surface temperature anomalies (land only, °C) from January 1990 - present, computed as departures from the 1971–2000 base period means.

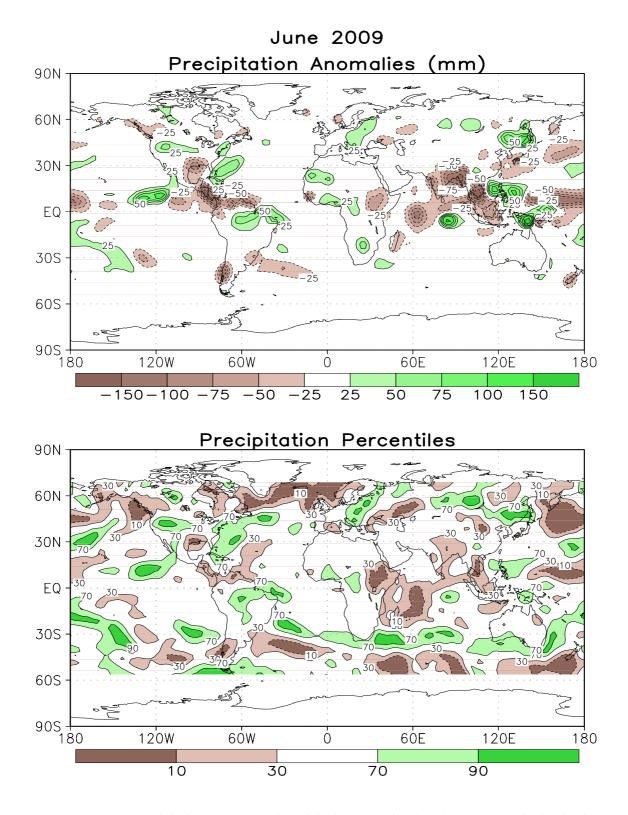


FIGURE E3. Anomalous precipitation (mm, top) and precipitation percentiles based on a Gamma distribution fit to the 1979–2000 base period data (bottom) for JUN 2009. Data are obtained from a merge of raingauge observations and satellite-derived precipitation estimates (Janowiak and Xie 1999, *J. Climate*, **12**, 3335–3342). Contours are drawn at 200, 100, 50, 25, -25, -50, -100, and -200 mm in top panel. Percentiles are not plotted in regions where mean monthly precipitation is <5mm/month.

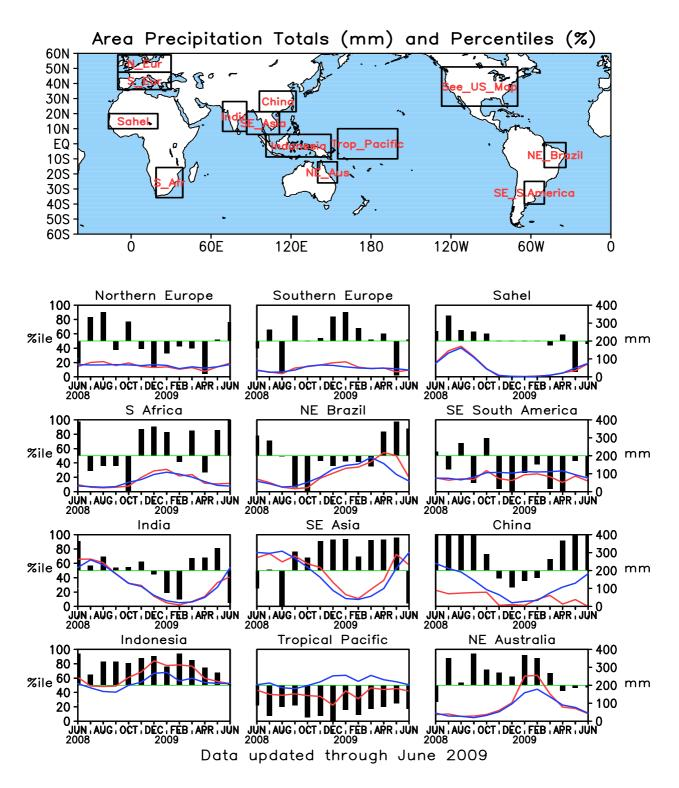


FIGURE E4. Areal estimates of monthly mean precipitation amounts (mm, solid lines) and precipitation percentiles (%, bars) for the most recent 13 months obtained from a merge of raingauge observations and satellite-derived precipitation estimates (Janowiak and Xie 1999, *J. Climate*, **12**, 3335–3342). The monthly precipitation climatology (mm, dashed lines) is from the 1979–2000 base period monthly means. Monthly percentiles are not shown if the monthly mean is less than 5 mm.

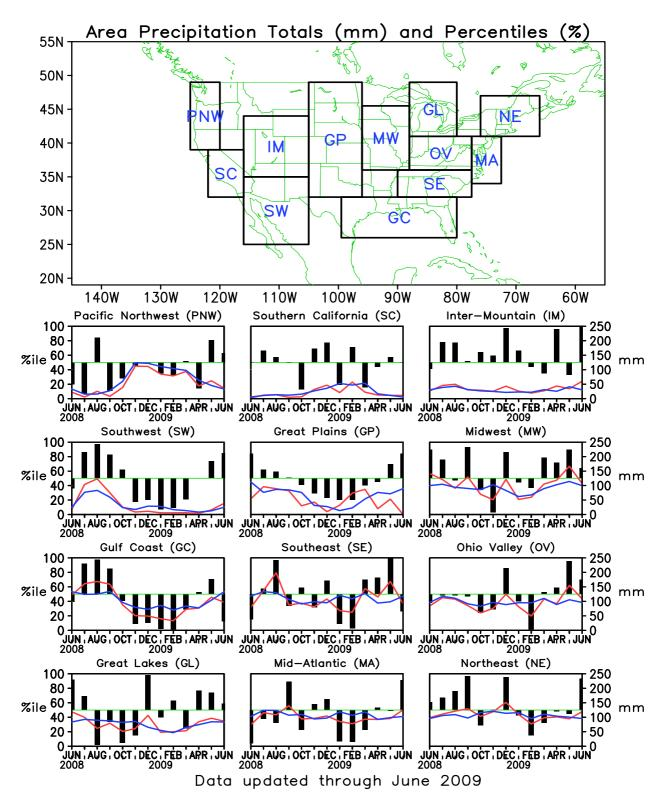
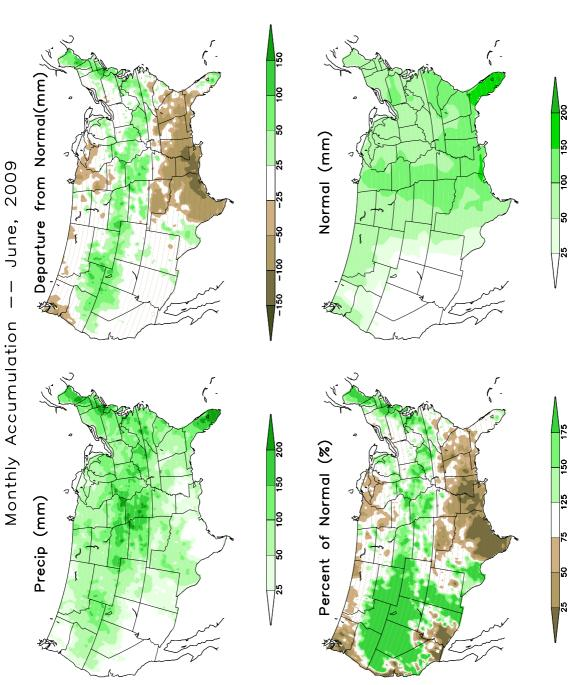
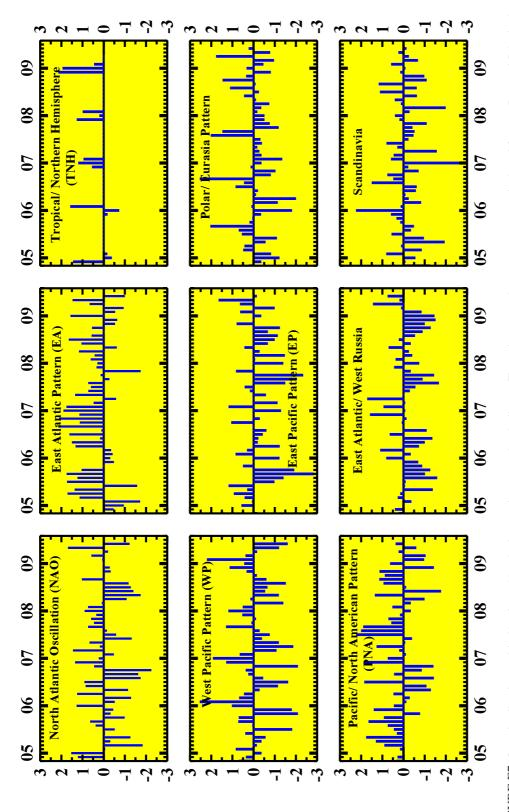


FIGURE E5. Areal estimates of monthly mean precipitation amounts (mm, solid lines) and precipitation percentiles (%, bars) for the most recent 13 months obtained from a merge of raingauge observations and satellite-derived precipitation estimates (Janowiak and Xie 1999, *J. Climate*, **12**, 3335–3342). The monthly precipitation climatology (mm, dashed lines) is from the 1979–2000 base period monthly means. Monthly percentiles are not shown if the monthly mean is less than 5 mm.







Component Analysis (RPCA) applied to monthly standardized 500-hPa height anomalies during January 1950 – December 2000. To obtain these month period centered on that month: [i.e., The July modes are calculated from the June, July, and August standardized monthly anomalies]. A standardized for each pattern and calendar month independently. No index value exists when the teleconnection pattern does not appear as one FIGURE E7. Standardized monthly Northern Hemisphere teleconnection indices. The teleconnection patterns are calculated from a Rotated Principal Varimax spatial rotation of the ten leading un-rotated modes for each calendar month results in 120 rotated modes (12 months x 10 modes per month) that yield ten primary teleconnection patterns. The teleconnection indices are calculated by first projecting the standardized monthly The indices are then solved for simultaneously using a Least-Squares approach. In this approach, the indices are the solution to the Least-Squares system of equations which explains the maximum spatial structure of the observed height anomaly field during the month. The indices are then patterns, ten leading un-rotated modes are first calculated for each calendar month by using the monthly height anomaly fields for the threeanomalies onto the teleconnection patterns corresponding to that month (eight or nine teleconnection patterns are seen in each calendar month) of the ten leading rotated EOF's valid for that month.

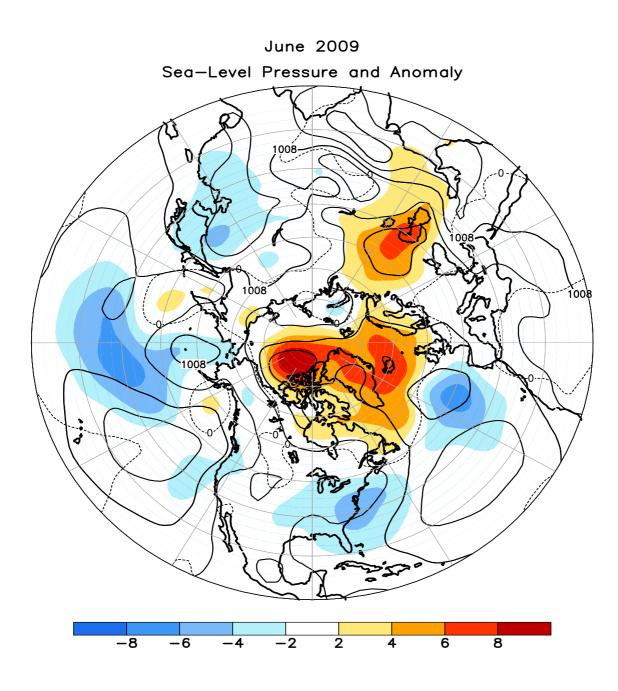


FIGURE E8. Northern Hemisphere mean and anomalous sea level pressure (CDAS/Reanalysis) for JUN 2009. Mean values are denoted by solid contours drawn at an interval of 4 hPa. Anomaly contour interval is 2 hPa with values less (greater) than -2 hPa (2 hPa) indicated by dark (light) shading. Anomalies are calculated as departures from the 1979-95 base period monthly means.

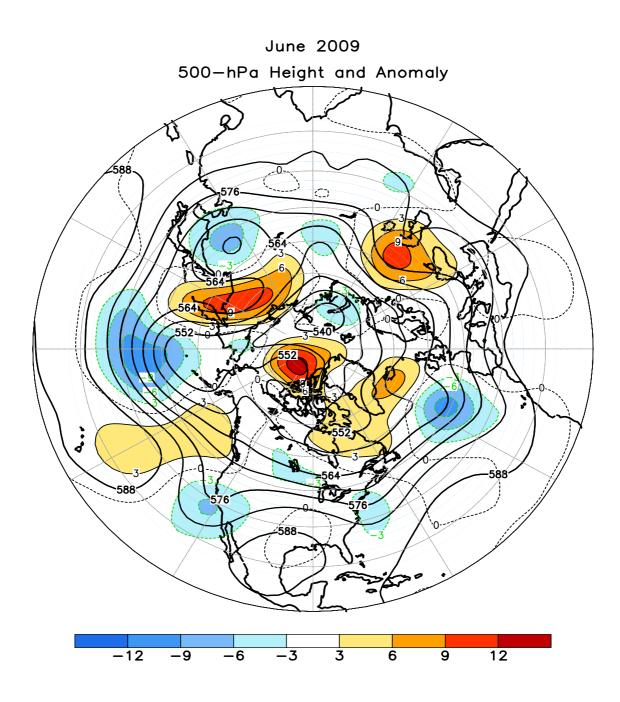


FIGURE E9. Northern Hemisphere mean and anomalous 500-hPa geopotential height (CDAS/Reanalysis) for JUN 2009. Mean heights are denoted by solid contours drawn at an interval of 6 dam. Anomaly contour interval is 3 dam with values less (greater) than -3 dam (3 dam) indicated by dark (light) shading. Anomalies are calculated as departures from the 1979-95 base period monthly means.

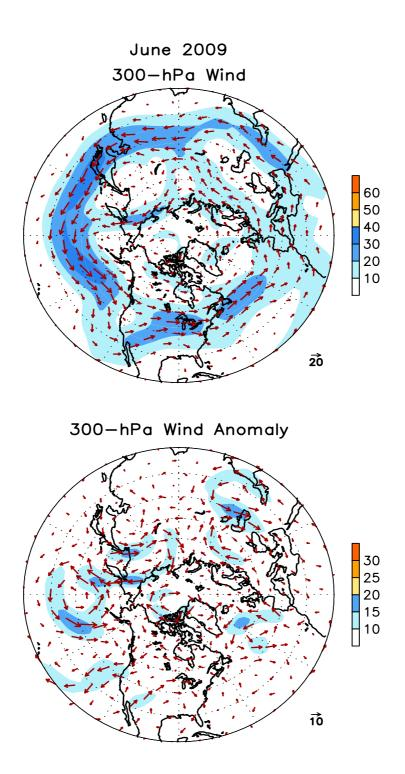


FIGURE E10. Northern Hemisphere mean (left) and anomalous (right) 300-hPa vector wind (CDAS/Reanalysis) for JUN 2009. Mean (anomaly) isotach contour interval is 10 (5) ms⁻¹. Values greater than 30 ms⁻¹ (left) and 10 ms⁻¹ (rights) are shaded. Anomalies are departures from the 1979-95 base period monthly means.

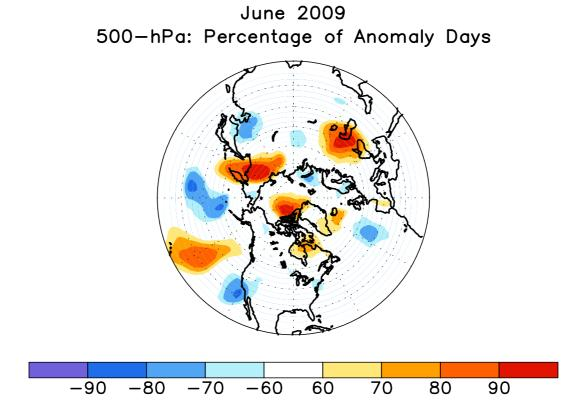


FIGURE E11. Northern Hemisphere percentage of days during JUN 2009 in which 500-hPa height anomalies greater than 15 m (red) and less than -15 m (blue) were observed. Values greater than 70% are shaded and contour interval is 20%.

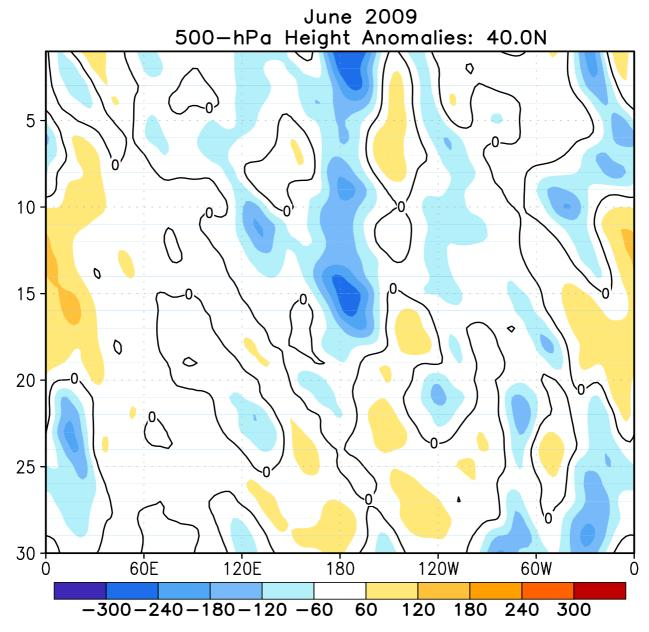


FIGURE E12. Northern Hemisphere: Daily 500-hPa height anomalies for JUN 2009 averaged over the 5° latitude band centered on 40°N. Positive values are indicated by solid contours and dark shading. Negative values are indicated by dashed coutours and light shading. Contour interval is 60 m. Anomalies are departures from the 1979-95 base period daily means.

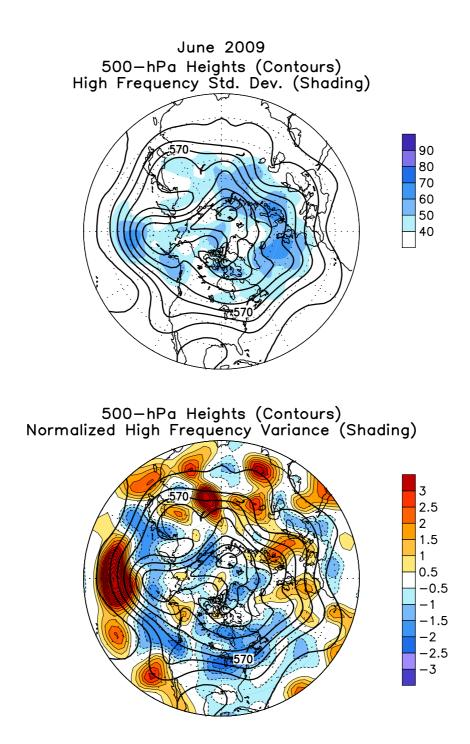


FIGURE E13. Northern Hemisphere 500-hPa heights (thick contours, interval is 6 dam) overlaid with (Top) Standard deviation of 10-day high-pass (HP) filtered height anomalies and (Bottom) Normalized anomalous variance of 10-day HP filtered height anomalies. A Lanczos filter is used to calculate the HP filtered anomalies. Anomalies are departures from the 1979-2000 daily means.

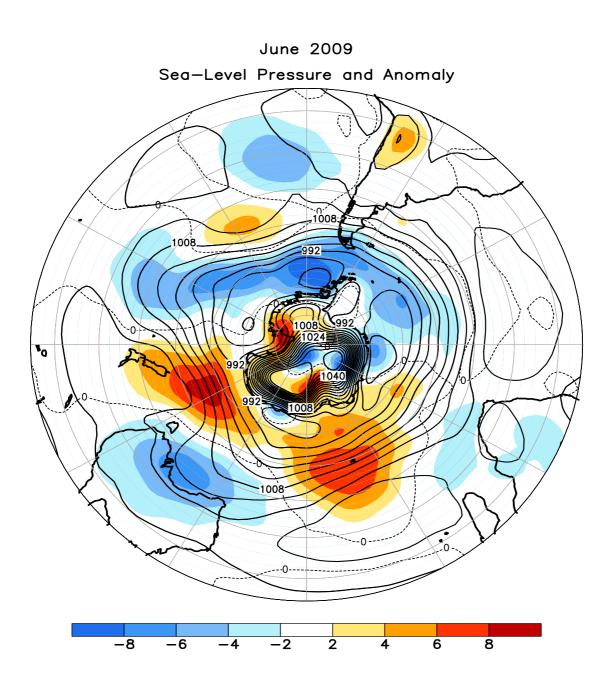


FIGURE E14. Southern Hemisphere mean and anomalous sea level pressure(CDAS/Reanalysis) for JUN 2009. Mean values are denoted by solid contours drawn at an interval of 4 hPa. Anomaly contour interval is 2 hPa with values less (greater) than -2 hPa (2 hPa) indicated by dark (light) shading. Anomalies are calculated as departures from the 1979-95 base period monthly means.

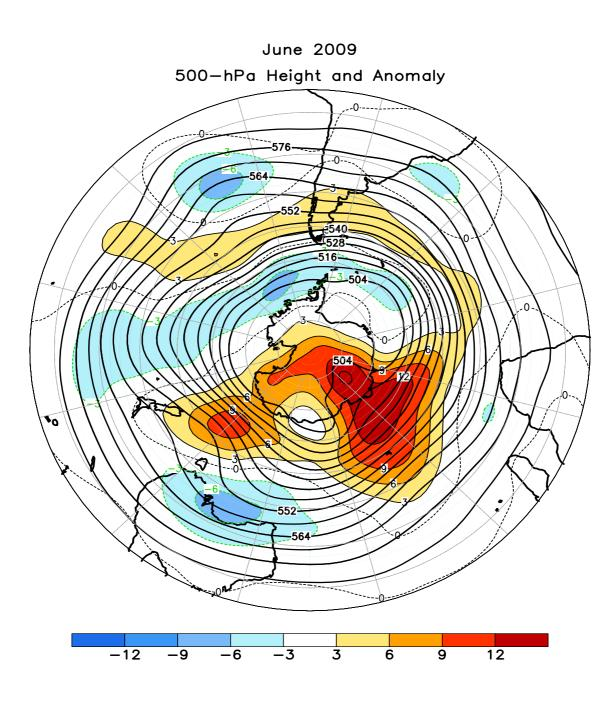


FIGURE E15. Southern Hemisphere mean and anomalous 500-hPa geopotential height (CDAS/Reanalysis) for JUN 2009. Mean heights are denoted by solid contours drawn at an interval of 6 dam. Anomaly contour interval is 3 dam with values less (greater) than -3 dam (3 dam) indicated by dark (light) shading. Anomalies are calculated as departures from the 1979-95 base period monthly means.

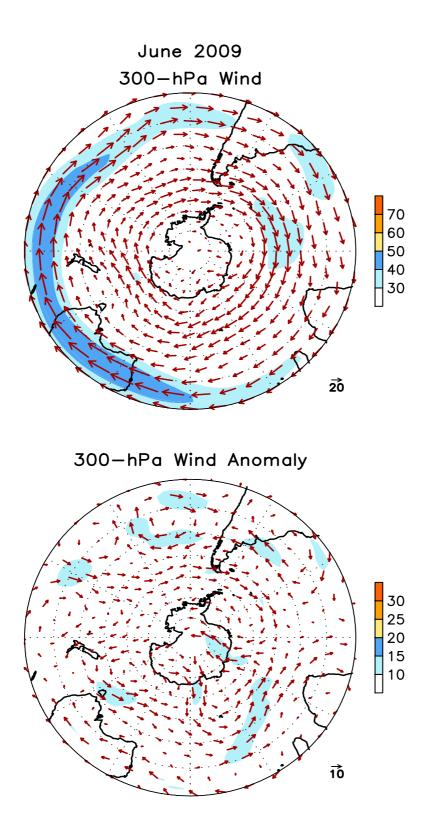


FIGURE E16. Southern Hemisphere mean (left) and anomalous (right) 300-hPa vector wind (CDAS/Reanalysis) for JUN 2009. Mean (anomaly) isotach contour interval is 10 (5) ms⁻¹. Values greater than 30 ms⁻¹ (left) and 10 ms⁻¹ (rights) are shaded. Anomalies are departures from the 1979-95 base period monthly means.

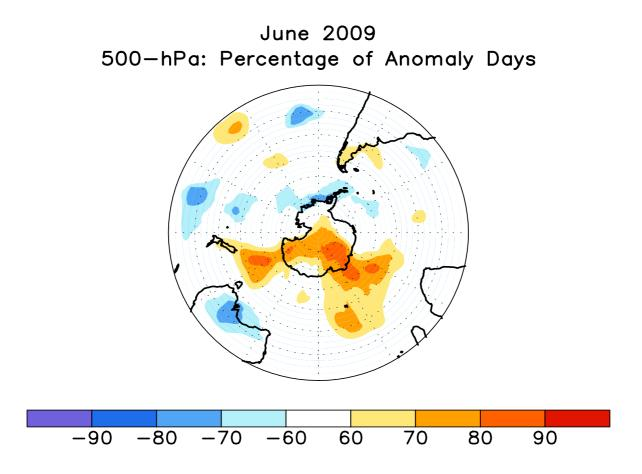


FIGURE E17. Southern Hemisphere percentage of days during JUN 2009 in which 500-hPa height anomalies greater than 15 m (red) and less than -15 m (blue) were observed. Values greater than 70% are shaded and contour interval is 20%.

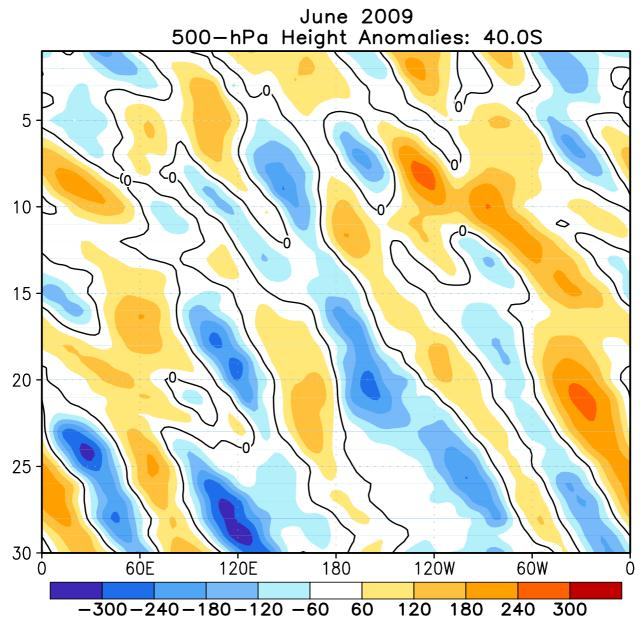


FIGURE E18. Southern Hemisphere: Daily 500-hPa height anomalies for JUN 2009 averaged over the 5° latitude band centered on 40°S. Positive values are indicated by solid contours and dark shading. Negative values are indicated by dashed coutours and light shading. Contour interval is 60 m. Anomalies are departures from the 1979-95 base period daily means.

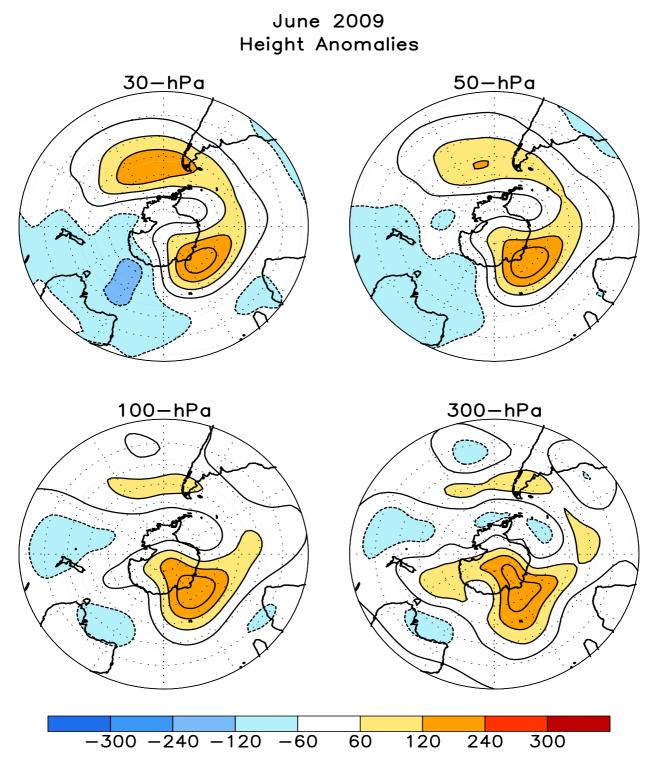


FIGURE S1. Stratospheric height anomalies (m) at selected levels for JUN 2009. Positive values are indicated by solid contours and dark shading. Negative values are indicated by dashed contours and light shading. Contour interval is 60 m. Anomalies are calculated from the 1979–95 base period means. Winter Hemisphere is shown.

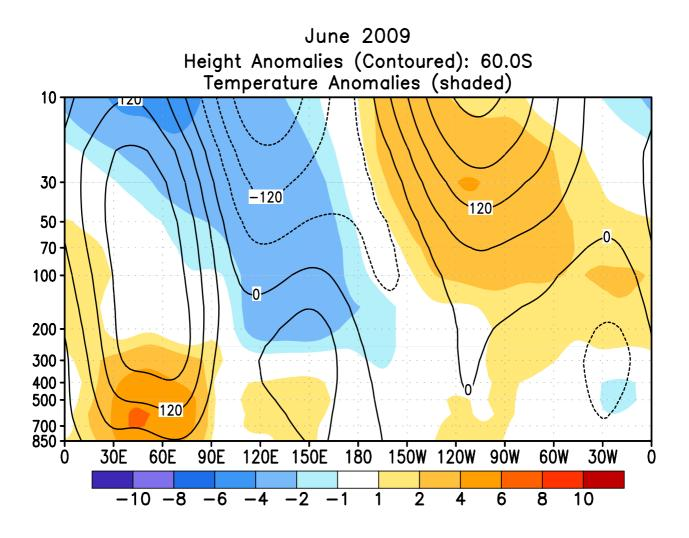


FIGURE S2. Height-longitude sections during JUN 2009 for height anomalies (contour) and temperature anomalies (shaded). In both panels, positive values are indicated by solid contours and dark shading, while negative anomalies are indicated by dashed contours and light shading. Contour interval for height anomalies is 60 m and for temperature anomalies is 2°C. Anomalies are calculated from the 1979–95 base period monthly means. Winter Hemisphere is shown.

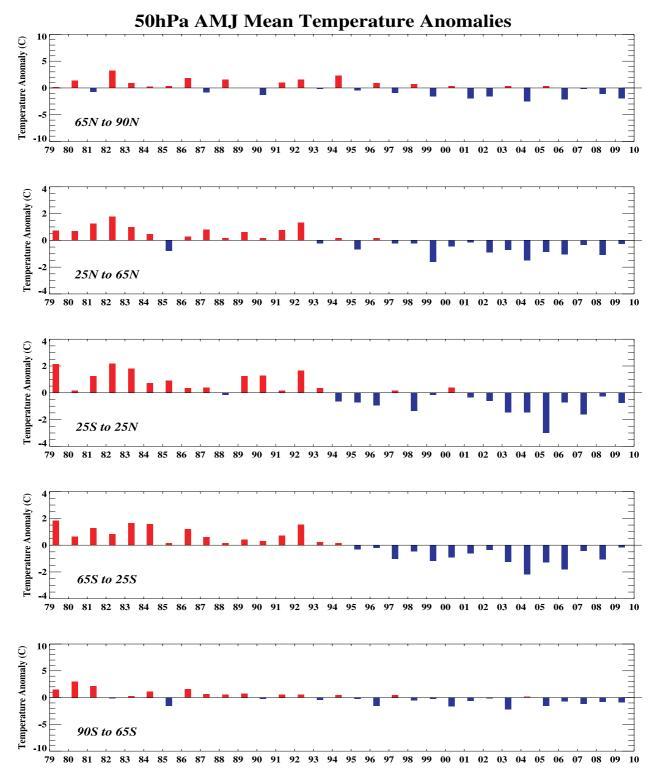


FIGURE S3. Seasonal mean temperature anomalies at 50-hPa for the latitude bands 65°–90°N, 25°–65°N, 25°N–25°S, 25°– 65°S, 65°–90°S. The seasonal mean is comprised of the most recent three months. Zonal anomalies are taken from the mean of the entire data set.

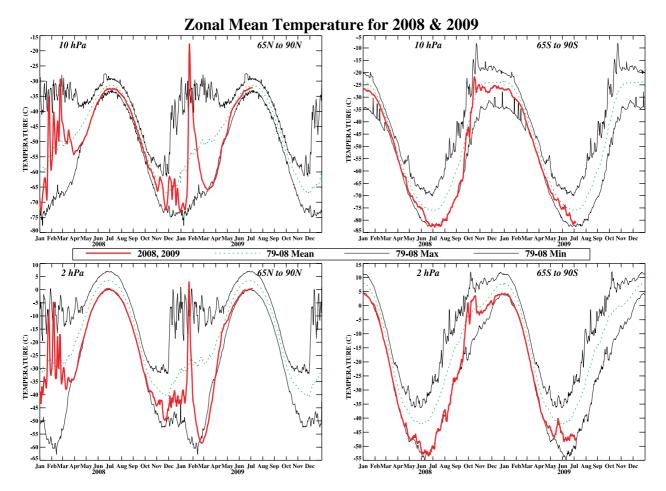
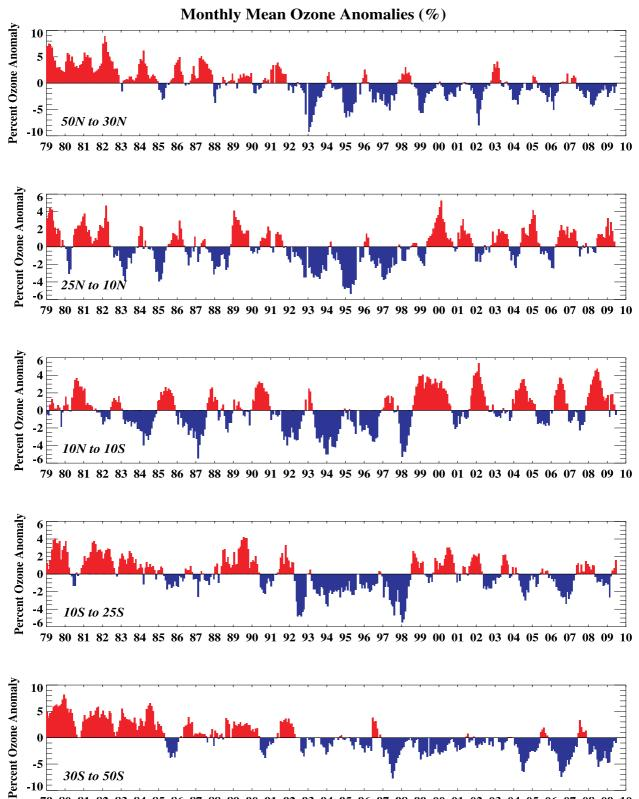
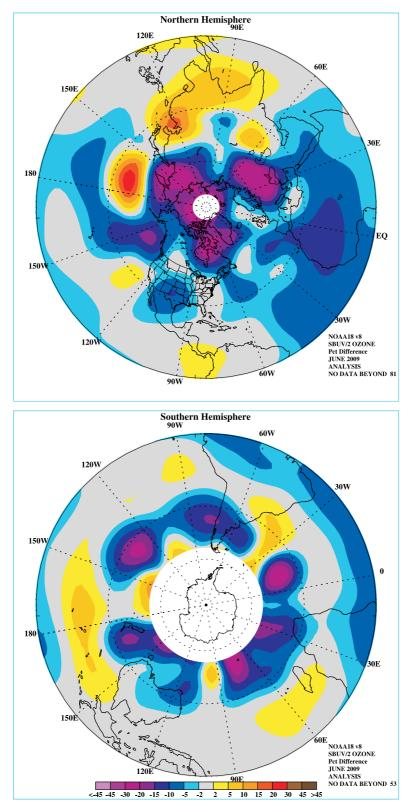


FIGURE S4. Daily mean temperatures at 10-hPa and 2-hPa (thick line) in the region 65°–90°N and 65°–90°S for the past two years. Dashed line depicts the 1979–99 base period daily mean. Thin solid lines depict the daily extreme maximum and minimum temperatures.



79 80 81 82 83 84 85 86 87 88 89 90 91 92 93 94 95 96 97 98 99 00 01 02 03 04 05 06 07 08 09 10 FIGURE S5. Monthly ozone anomalies (percent) from the long term monthly means for five zones: 50N-30N (NH mid-latitudes), 25N-10N (NH tropical surf zone), 10N-10S (Equatorial-QBO zone), 10S-25S (SH tropical surf zone), and 30S-50S (SH mid-latitudes). The long term monthly means are determined from the entire data set beginning in 1979.



JUNE PERCENT DIFF (2009 - AVG(79-86))

FIGURE S6. Northern (top) and Southern (bottom) Hemisphere total ozone anomaly (percent difference from monthly mean for the period 1979–86). The region near the winter pole has no SBUV/2 data.

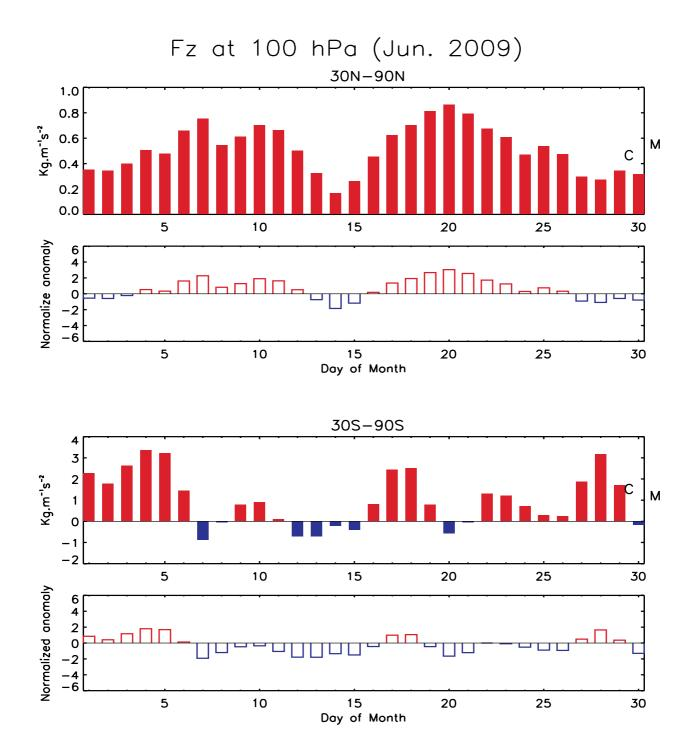


FIGURE S7. Daily vertical component of EP flux (which is proportional to the poleward transport of heat or upward transport of potential energy by planetary wave) at 100 hPa averaged over (top) 30°N–90°N and (bottom) 30°S–90°S for JUN 2009. The EP flux unit (kg m⁻¹ s⁻²) has been scaled by multiplying a factor of the Brunt Vaisala frequency divided by the Coriolis parameter and the radius of the earth. The letter 'M' indicates the current monthly mean value and the letter 'C' indicates the climatological mean value. Additionally, the normalized departures from the monthly climatological EP flux values are shown.

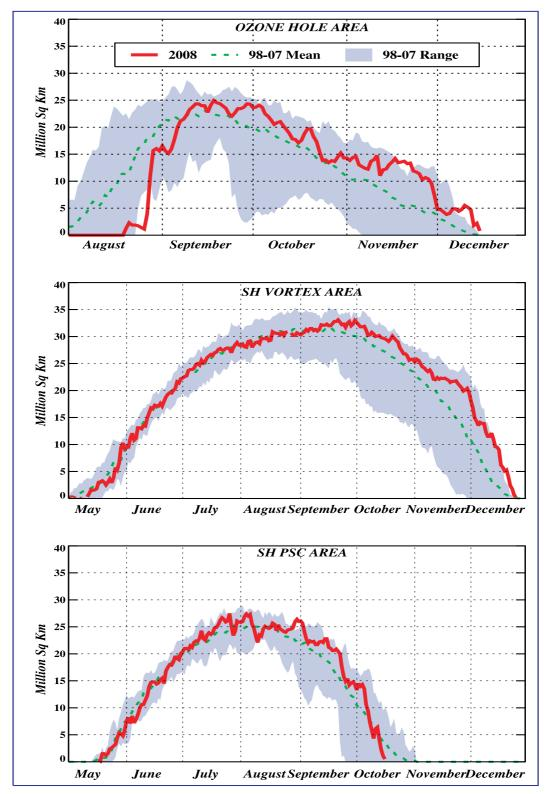


FIGURE S8. Daily time series showing the size of the NH polar vortex (representing the area enclosed by the 32 PVU contour on the 450K isentropic surface), and the areal coverage of temperatures < -78C on the 450K isentropic surface.

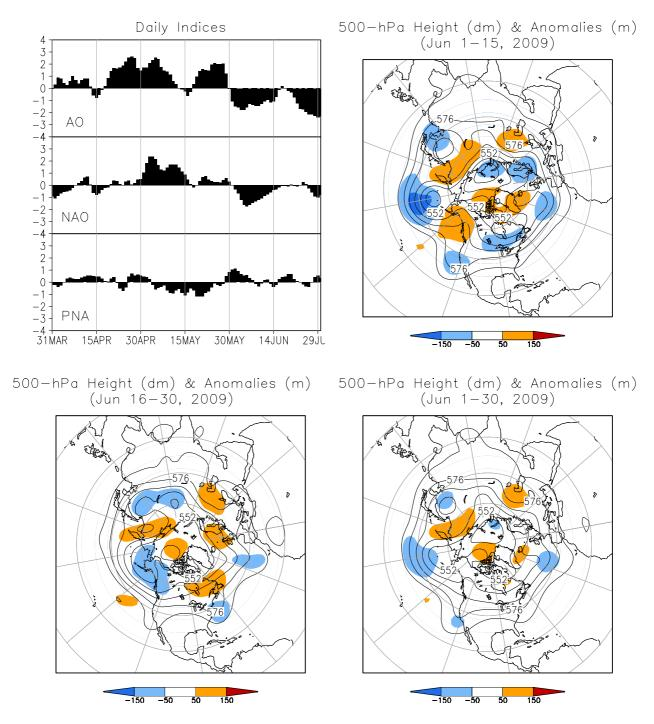


FIGURE A2.1. (a) Daily amplitudes of the Arctic Oscillation (AO) the North Atlantic Oscillation (NAO), and the Pacific-North American (PNA) pattern. The pattern amplitudes for the AO, (NAO, PNA) are calculated by projecting the daily 1000-hPa (500-hPa) height anomaly field onto the leading EOF obtained from standardized time- series of daily 1000-hPa (500-hPa) height for all months of the year. The base period is 1979–2000.

(b-d) Northern Hemisphere mean and anomalous 500-hPa geopotential height (CDAS/Reanalysis) for selected periods during JUN 2009 are shown in the remaining 3 panels. Mean heights are denoted by solid contours drawn at an interval of 8 dam. Dark (light) shading corresponds to anomalies greater than 50 m (less than -50 m). Anomalies are calculated as departures from the 1979–95 base period daily means.

SSM/I Snow Cover for Jun 2009 anomaly based on departure from 1987-2006 baseline

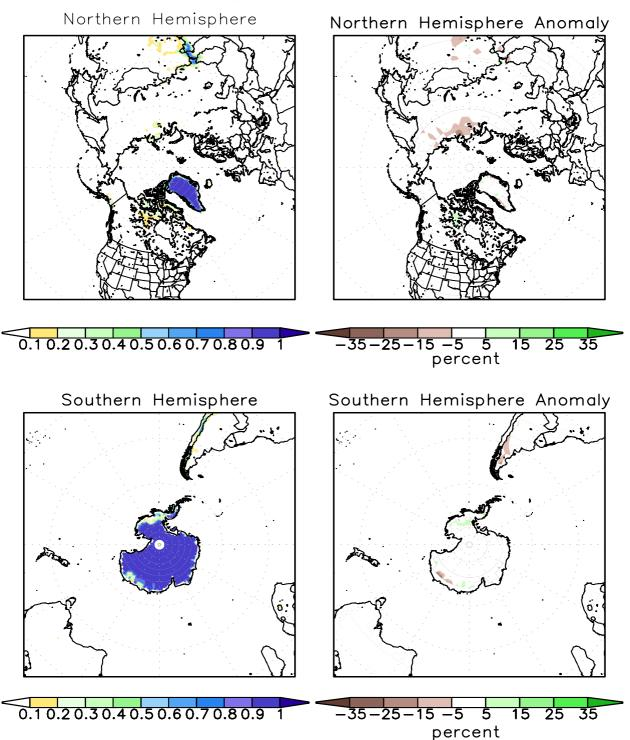


FIGURE A2.2. SSM/I derived snow cover frequency (%) (left) and snow cover anomaly (%) (right) for the month of JUN 2009 based on 1987 - 2006 base period for the Northern Hemisphere (top) and Southern Hemisphere (bottom). It is generated using the algorithm described by Ferraro et. al, 1996, Bull. Amer. Meteor. Soc., vol 77, 891-905.